haematologica
Journal of The Ferrata Storti Foundation

Halting the vicious cycle within the multiple myeloma ecosystem: blocking JAM-A on bone marrow endothelial cells restores the angiogenic homeostasis and suppresses tumor progression

by Antonio G. Solimando, Matteo C. Da Vià, Patrizia Leone, Paola Borrelli, Giorgio A. Croci, Paula Tabares, Andreas Brandl, Giuseppe Di Lernia, Francesco P. Bianchi, Silvio Tafuri, Torsten Steinbrunn, Alessandra Balduini, Assunta Melaccio, Simona De Summa, Antonella Argentiero, Hilka Rauert-Wunderlich, Maria A. Frassanito, Paolo Ditonno, Erik Henke, Wolfram Klapper, Roberto Ria, Carolina Terragna, Leo Rasche, Andreas Rosenwald, K. Martin Kortüm, Michele Cavo, Domenico Ribatti, Vito Racanelli, Hermann Einsele, Angelo Vacca, and Andreas Beilhack

Haematologica 2020 [Epub ahead of print]

Citation: Antonio G. Solimando, Matteo C. Da Vià, Patrizia Leone, Paola Borrelli, Giorgio A. Croci, Paula Tabares, Andreas Brandl, Giuseppe Di Lernia, Francesco P. Bianchi, Silvio Tafuri, Torsten Steinbrunn, Alessandra Balduini, Assunta Melaccio, Simona De Summa, Antonella Argentiero, Hilka Rauert-Wunderlich, Maria A. Frassanito, Paolo Ditonno, Erik Henke, Wolfram Klapper, Roberto Ria, Carolina Terragna, Leo Rasche, Andreas Rosenwald, K. Martin Kortüm, Michele Cavo, Domenico Ribatti, Vito Racanelli, Hermann Einsele, Angelo Vacca, and Andreas Beilhack. Halting the vicious cycle within the multiple myeloma ecosystem: blocking JAM-A on bone marrow endothelial cells restores the angiogenic homeostasis and suppresses tumor progression.
Haematologica. 2020; 105:xxx
doi:10.3324/haematol.2019.239913

Halting the vicious cycle within the multiple myeloma ecosystem: blocking JAM-A on bone marrow endothelial cells restores the angiogenic homeostasis and suppresses tumor progression.

Antonio G. Solimando[1,2,3], Matteo C. Da Viá[1], Patrizia Leone[3], Paola Borrelli[4], Giorgio A. Croci[5,6], Paula Tabares[1,7], Andreas Brandl[1,7], Giuseppe Di Lernia[3], Francesco P. Bianchi[8], Silvio Tafuri[8], Torsten Steinbrunn[1], Alessandra Balduini[9,10], Assunta Melaccio[3], Simona De Summa[11], Antonella Argentiero[2], Hilka Rauert-Wunderlich[12], Maria A. Frassanito[3], Paolo Ditonno[2], Erik Henke[13], Wolfram Klapper[5], Roberto Ria[3], Carolina Terragna[14], Leo Rasche[1], Andreas Rosenwald[12], K. Martin Kortüm[1], Michele Cavo[14], Domenico Ribatti[15], Vito Racanelli[3*], Hermann Einsele[1*], Angelo Vacca[3‡], and Andreas Beilhack[1,7‡].

[1]*Department of Medicine II, University Hospital of Würzburg, Würzburg, Germany*
[2]*IRCCS Istituto Tumori "Giovanni Paolo II", Bari, Italy*
[3]*Department of Biomedical Sciences and Human Oncology, Unit of Internal Medicine "Guido Baccelli", University of Bari Aldo Moro Medical School, Bari, Italy*
[4]*Unit of Biostatistics and Clinical Epidemiology, Department of Public Health, Experimental and Forensic Medicine, University of Pavia, Pavia, Italy*
[5]*Department of Pathology, Hematopathology Section and Lymph Node Registry, University of Kiel/University Hospital Schleswig-Holstein, Kiel, Germany*
[6]*Pathology Unit, Department of Pathophysiology and Transplantation, University of Milan and Fondazione IRCCS, Ca' Granda, Milan, Italy*
[7]*Interdisciplinary Center for Clinical Research Laboratory, University Hospital of Würzburg, Würzburg, Germany*
[8]*Section of Hygiene, Department of Biomedical Science and Human Oncology, University of Aldo Moro Medical School, Bari, Italy*
[9]*Department of Molecular Medicine, University of Pavia, Pavia, Italy*
[10]*Department of Biomedical Engineering, Tufts University, Medford, MA, USA*
[11]*Molecular Diagnostics and Pharmacogenetics Unit, IRCCS Istituto Tumori "Giovanni Paolo II", Bari, Italy*
[12]*Institute of Pathology, University of Würzburg, Würzburg, Germany*
[13]*Institute of Anatomy and Cell Biology, Julius-Maximilians Universität Würzburg, Würzburg, Germany*
[14]*Institute of Hematology "L. and A. Seràgnoli", Bologna, Italy*
[15]*Department of Basic Medical Sciences, Neurosciences and Sensory Organs, University of Bari Aldo Moro Medical School, Bari, Italy*

*These authors contributed equally to this study.

‡These authors contributed equally to the conception and design of this study.

Correspondence to:
Prof. Andreas Beilhack, M.D.
Department of Internal Medicine II
University Hospital Würzburg, Germany 97078
Telephone: +49-931-201 44040
Fax: +49-931-201 27639
E-mail: beilhack_a@ukw.de
The authors declare no conflict of interest

Word counts: 200 (abstract); 4044 (main text)

Abstract

Interactions of malignant multiple myeloma (MM) plasma cells (MM-cells) with the microenvironment control MM-cell growth, survival, drug-resistance and dissemination. As in MM microvascular density increases in the bone marrow (BM), we investigated whether BM MM endothelial cells (MMECs) control disease progression via the junctional adhesion molecule A (JAM-A). Membrane and cytoplasmic JAM-A levels were upregulated in MMECs in 111 newly diagnosed (NDMM) and 201 relapsed-refractory (RRMM) patients compared to monoclonal gammopathy of undetermined significance (MGUS) and healthy controls. Elevated membrane expression of JAM-A on MMECs predicted poor clinical outcome. Mechanistically, addition of recombinant JAM-A to MMECs increased angiogenesis whereas its inhibition impaired angiogenesis and MM growth in 2D and 3D *in vitro* cell culture and chorioallantoic membrane-assays. To corroborate these findings, we treated MM bearing mice with JAM-A blocking mAb and demonstrated impaired MM progression corresponding to decreased MM-related vascularity. These findings support JAM-A as an important mediator of MM progression through facilitating MM-associated angiogenesis. Collectively, elevated JAM-A expression on bone marrow endothelial cells is an independent prognostic factor for patient survival in both NDMM and RRMM. Blocking JAM-A restricts angiogenesis *in vitro*, *in embrio* and *in vivo* and represents a suitable druggable molecule to halt neoangiogenesis and MM progression.

Introduction

Junctional adhesion molecule-A (JAM-A), also known as JAM-1, CD321, *F11R*, belongs to the immunoglobulin superfamily.[1] In healthy tissues, JAM-A regulates cell growth and differentiation, while its aberrant expression or deregulation confers a more aggressive phenotype with poor prognosis in different types of human cancers[1], including multiple myeloma (MM)[2], breast, lung, brain and head and neck cancer.[3]

JAM-A over-activation results either from upregulation or aberrant dimerization, driving the receptor in a state of constitutive signal transmission, or from excessive release of JAM-A ligands by normal and tumor cells into the microenvironment.[4] Membrane-bound JAM-A and its soluble form (sJAM-A) can form homophilic interactions and also heterophilic interactions[1] with lymphocyte function-associated antigen 1 (LFA-1), afadin (AFDN), calcium/calmodulin-dependent serine protein kinase (CASK) and tight junction protein-1 (TJP1) with high receptor/ligand binding affinities.[5] These interactions trigger JAM-A downstream signaling pathways involved in the regulation of tumor cell survival, growth, angiogenesis and dissemination.[6]

JAM-A inhibition can be achieved by direct blocking of both the ligand-binding site on the extracellular receptor domain with monoclonal antibodies (mAb)[7] and indirectly with small-molecule inhibitors.[8] Moreover, neutralizing the sJAM-A[9] released into the microenvironment can prevent JAM-A activation.[10]

JAM-A plays a pivotal role in endothelial cell physiology[6] and pathology.[2] Although JAM-A function in tumorigenesis has been investigated in solid tumors[3], and its angiogenic role has been shown in pancreatic islet carcinoma[11], data on JAM-A related angiogenesis in hematologic neoplasms remains elusive. Since BM neovascularization favors MM progression[12], we investigated whether JAM-A can drive angiogenesis in MM[13] contributing to MM disease progression.[2]

We quantified JAM-A surface expression on 312 MM patient's BM-derived endothelial cells (MMECs) and demonstrated that JAM-A^{high} MMECs strongly correlate with poor survival both in newly diagnosed (NDMM) and relapsed/refractory (RRMM) patients. Mechanistically, adding recombinant JAM-A protein to MM-cells increased angiogenesis in both 2D and 3D models. Conversely, blocking JAM-A impaired MM related angiogenesis. To corroborate these findings, we treated MM bearing mice with JAM-A blocking mAb and observed impaired MM progression and decreased MM vascularity.

Methods

Patients

Patients fulfilling the International Myeloma Working Group diagnostic criteria[14] for NDMM (n=111), relapsed/refractory patients[15] (RRMM) (n=201) and monoclonal gammopathy of undetermined significance (MGUS) (n=35) were included in this study. Patient characteristics and genetics risk stratification are provided in **Supplementary Table 1 and 2**. The study was approved by the

Ethical Committee of the Bari and Würzburg University Hospitals (reference number 5145 and 76/13), and all patients provided their informed consent following the Declaration of Helsinki, (detailed in Supplementary Methods).

Cell lines and cultures procedures

RPMI-8226, OPM-2 and HUVECs cells were cultured as described.[3] MM-cells were co-cultured with MMECs (4×10^5) at a 1:1 and 1:5 cell ratios for 24 hours with or without an inserted transwell (0.4 µm pore size; Costar, Cambridge, MA, USA) (detailed in Supplementary Methods).

Chick chorioallantoic membrane (CAM) assay

Fertilized chicken eggs were incubated at 37°C at constant humidity. On day 8, sterilized gelatin sponges adsorbed with MMECs conditioned medium (CM) or medium obtained by treatment of MMECs with sJAM-A (100 ng/mL), with or without α-JAM-A mAb were implanted on the top of the CAM (detailed in Supplementary Methods).

MM xenograft mouse models

Twenty female 8- to 10-week-old NOD.CB17-Prkdcscid/NCrHsd mice (NOD-SCID, Envigo, Huntingdon, UK) were injected intratibially with 2×10^5 RPMI-8226 cells suspended in PBS. Mice were treated with the α-JAM-A mAb (Sigma-Aldrich, St. Louis, MO, USA, mouse monoclonal clone J10.4) recognizing the distal membrane extracellular domain of JAM-A.

Twenty female 6- to 8-week-old NOD-SCID mice were injected subcutaneously (s.c.) into the right-hand flank with 1×10^7 RPMI-8226 cells suspended in 200 µL RPMI-1640 medium and 200 µL Matrigel™ as described[16] (detailed in Supplementary Methods).

Functional *in vitro* assays

Wound-healing and Matrigel™ angiogenesis assays were performed as previously described (detailed in Supplementary Methods).

Protein expression studies and Reverse transcriptase PCR, real-time RT-PCR

Western blot, ELISA, human angiogenesis array real-time RT-PCR were performed according to manufacturer's instructions (detailed in Supplementary Methods).

Immunohistochemistry

Details are supplied in Supplementary Methods.

***In silico* analysis from the** CoMMpass study dataset

Details are supplied in Supplementary Methods.

Statistical analysis

Descriptive analysis was carried out using median and interquartile range for the quantitative variables and percentages values for the qualitative ones.

Normality distribution was tested using the Shapiro-Wilk test. Membrane MMECs JAM-A expression levels (mean fluorescence intensity - MFI obtained in FACS) were dichotomized into two classes, JAM-A$^{high/low}$, choosing the median as class boundary (detailed in Supplementary Methods). Moreover, for further confirmatory survival analysis quartile ranges based model has been implemented (detailed in Supplementary Methods).

Results

Elevated JAM-A expression on BM primary MMECs correlates with poor prognosis in both NDMM and RRMM

First, we compared the JAM-A expression in MMECs and MGECs (**Figure 1A**). JAM-A mRNA expression in MMECs significantly exceeded JAM levels in MGECs (1.8 fold-change, *P*<.0001) and of healthy endothelial cells (**Supplementary Figure 1A**). Subsequent Western Blot (WB) analysis confirmed that MMECs significantly upregulated JAM-A protein expression in comparison to MGECs (*P*<.0001, **Figure 1B**).

Because JAM-A had proven as a prominent adhesion molecule on MM cells previously[2] and is also known to form homophilic interactions[1], we investigated whether JAM-A expression on the vascular microenvironment affects disease outcome. To this end, we enrolled 312 patients, 111 with newly diagnosed MM (NDMM) and 201 with relapsed/refractory (RRMM) disease. Employing flow cytometry on MMECs we divided newly diagnosed MM patients based on JAM-A^{high} and JAM-A^{low} MMEC surface expression (**Figure 1C)**. Immunohistochemical analyses of BM trephines corroborated these findings (**Figure 1D, Supplementary Figure 1B, C**). Notably, OS was significantly shorter in patients with JAM-A^{high} MMECs than in patients with JAM-A^{low} MMECs (**Figure 1E upper panel**) [JAM-A^{high} MMEC group median not reached (NR) *vs.* JAM-A^{low} MMEC group 78 months (hazards ratio-HR=9.14, 95% CI 2.8–29.76), *P*<.001; χ^2_{LR}=20.11; *P*<.0001]. Strikingly, these results maintained significant also in the multivariate analysis (HR=9.11, 95% CI 2.79–29.76), *P* <.001) (**Figure 1E lower panel**); concerning the PFS, only the renal impairment displayed a significant impact in univariate as well as in multivariate analysis (HR=1.64, 95% CI 1.09–2.47, *P*=.017); MMECs JAM-A expression levels did not influence risk of progression in NDMM (data not shown). Thus, JAM-A overexpression on MMECs represents a risk factor for a shorter OS in NDMM.

Next, we interrogated a 201 RRMM cohort with flow cytometry. Within these relapsed/refractory patients, JAM-A^{high} MMECs represented an independent poor prognostic factor for OS and also for PFS (**Figure 2A-B)**. Survival differed significantly in patients with JAM-A^{high} MMECs: the median

OS was 130 months in patients with JAM-A^{high} MMECs and not reached yet in those with JAM-A^{low} MMECs (**Figure 2A**, HR=2.96, 95% CI 1.36–6.37, *P*<.006; χ^2_{LR}=8.52; *P*=.0035).

In patients with JAM-A^{low} MMECs cells, the median PFS estimated was 27 months, while, in subjects with JAM-A^{high} MMECs the median PFS reached only 18.3 months (**Figure 2B**, HR=1.41, 95% CI 1.05-1.88; *P*=.019; χ^2_{LR}=5.78; *P*=.0162).

Multivariate analyses confirmed JAM-A^{high} MMECs as an independent significant risk factor for low OS (HR=2.39, 95% CI 1.09–5.28; *P*=.030) in much the same way were for R-ISS stage II (HR=5.34, 95% CI 1.24–22.97; *P*=.024) and III (HR=.57, 95% CI 1.25–34.54; *P*=.026) and chronic kidney disease (HR=2.12, 95% CI 1.00–4.52; *P*=.049) (**Figure 2C**). Cox stratified model implemented for PFS confirmed only high levels of membrane MMECs JAM-A as a statistically significant risk factor (HR=1.35, 95% CI 1.00–1.81; *P*=.044) stratified by chronic kidney disease (**Figure 2C**).

Interestingly, only the JAM-A^{high} MMECs kept significance in the multivariate model. Moreover, we found a significant association in RRMM setting between JAM-A^{high} MMECs and the R-ISS stage II and III (χ^2=17.4, *P*<.0001) and the risk of extramedullary dissemination (χ^2=7.04, *P*=.008). Thus, JAM-A surface expression on BM endothelial cells derived from MM patients exerted a strong and independent effect with a linear trajectory concerning OS impacted in both cohorts and an additive poor prognostic impact on PFS in the RRMM cohort. Additionally, we dissected the entire cohort (**Supplementary Figure 1D)** in quartile ranges of MMECs' surface expression and then compared the lowest (JAM-A^{Q1}) to the highest one (JAM-A^{Q4}). Strikingly, OS differed significantly in subjects from the JAM-A^{Q4}: the median OS was 88 months in JAM-A ^{Q4} patients and was not reached in JAM-A^{Q1} patients (HR=8.24, 95% CI 3.2–20.9, P<.0001; χ^2_{LR}=28.15; P<.0001). Interestingly, JAM-A^{Q4} MMECs kept significance in the multivariate Cox-model (HR=6.36, 95% CI 2.3–17.63; *P*<.001). This comparison further corroborated JAM-A positive *vs*. negative MMECs role in predicting poor clinical outcome in our cohort (**Supplementary Figure 1E, upper and lower panels**). The absence of a statistically significant impact on NDMM PFS is likely due to a more pronounced effect of JAM-A MMEC-expression in a more advanced MM stage. This suggests the importance of JAM-A within the BM microenvironment during disease progression.

MMECs enhance the JAM-A expression on MM-cells.

To address how interactions with MMECs functionally influence MM cell biology, we performed indirect and direct co-culture experiments of MMECs with MM-cell lines. JAM-A expression levels increased on MM-cells when co-cultured with MMECs (**Figure 3A, B).** We next exposed MM-cells to primary MMECs- or MGECs-derived culture media, respectively. Again, the JAM-A protein expression increased on MM-cells after exposure to MMECs medium compared to MGECs medium (**Figure 3C and D,** respectively). Results confirmed JAM-A upregulation upon direct co-culture experiments (**Supplementary Figure 2A**). Notably, only after direct co-culture MMECs

recapitulated the same behavior of MM-cells (**Supplementary Figure 2B**). Consistently, also soluble JAM-A (sJAM-A) levels increased after co-culture of MM with MMECs cells (**Supplementary Figure 2C**). Similar to RPMI-8226 cells, OPM-2 cells upregulated JAM-A after direct co-culture with MMECs (**Supplementary Figure 2D**), but not after indirect culture (data not shown). These data indicate that both cell-cell contact and soluble factors released by MMECs into the BM microenvironment upregulated JAM-A expression on MM-cells. MMECs JAM-A upregulation parallels this dynamic process, suggesting a vicious cycle, promoting MM growth by supporting angiogenesis.

JAM-A enhances angiogenesis in 2D and 3D conditions

We hypothesized that JAM-A upregulation during MM progression may enhance angiogenesis. To this end, we treated MMECs with increasing concentrations of human recombinant sJAM-A and measured different parameters[17] of angiogenesis.[18] To examine whether JAM-A directly affects spontaneous MMEC-migration, we performed experiments in 2D and 3D environments. Enhanced spontaneous MMECs migration was observed after 12 hours of sJAM-A treatment in a 2D *scratch assay* by counting migrating MMECs (**Figure 4A,** upper and lower panel). Blocking α-JAM-A abolished the enhanced MMECs migration (**Figure 4A,** upper panel) and reduced migrating MMECs numbers (**Figure 4A,** lower panel). In a 2D angiogenesis assay, sJAM-A treatment increased the endothelial structure complexity in terms of branching points and vessel lengths as angiogenesis parameters. Three hours after seeding, sJAM-A treatment resulted in a structured capillary network, while the control remained in a rudimentary stage of organization with small clumps of cells distributed on the Matrigel™ layer (**Figure 4B**, upper left quadrant). Furthermore, we tested the effect of JAM-A inhibition in MMECs by both siRNA and blocking α-JAM-A without adding sJAM-A (**Figure 4B,** lower left and upper right quadrants, respectively). Consistently, blocking JAM-A with a mAb impaired the capillary network formation and resulted in poorly skeletonized structures (**Figure 4B,** lower right quadrant). The observed down-modulation of MMEC migration, reduced number of branching points and vessel length occurred independent of cytotoxic effects, since JAM-A-neutralization did not affect MMEC survival (**Supplementary Figure 3A, left and right panels).**

Based on the 2D observations, we investigated whether JAM-A would influence structured MM-associated angiogenesis in a 3D CAM assay. CAMs were implanted with gelatin sponges loaded with either MMECs conditioned-medium as control (CTRL) or MMECs conditioned medium with sJAM-A (+sJAM-A), in presence or absence of a blocking α-JAM-A mAb. MMECs conditioned-medium stimulated new vessel formation in CAM[19] that was profoundly enhanced by adding sJAM-A. This effect could be selectively inhibited by treatment with a sJAM-A blocking antibody as treatment with a cocktail containing an isotype IgG1 control antibody (sJAM-A + ISO, middle panel) did not reduce vessel formation (**Figure 4C**).

To explore potential factors that enhance JAM-A mediated MM angiogenesis, we compared conditioned media from MMECs supplemented with sJAM-A before and after α-JAM-A treatment with an angiogenesis array (**Figure 4D and Supplementary Figure 3B**). sJAM-A strongly reduced anti-angiogenic and increased pro-angiogenic factors secreted by MMECs[16] such as plasminogen (PLG), fibroblast growth factor2 (FGF-2), insulin-like growth factor binding protein1 (IGFBP1) and vascular endothelial growth factors A and C (VEGFA, VEGFC). RT-PCR corroborated the proteomic findings and revealed sJAM-A-induced transcriptional upregulation of these factors and ligands (PLG and ENO1, JAM-A with LFA-1 and TJP1) (**Supplementary Figure 3C-L**). Moreover, because JAM-A can form homophilic interactions with JAM-A itself[1] as well as heterophilic interactions with LFA-1, TJP1, CAV1 and CASK, we investigated whether the expression of these ligands correlated with MM-MMECs interactions. Direct co-culture of RPMI-8226 and MMECs significantly increased LFA-1, CAV1 on MM-cells, whereas TJP1, CASK and ADAM17 expression levels decreased (**Supplementary Figure 3G-K**). Therefore, we tested if the induced gene expression was non-random, by testing further molecules involved in neoplastic angiogenesis processes[12], namely VEGFA, VEGFC, HGF, FGF[16] and Aurora Kinase A (AURKA)[20]; also in this case we found a significant VEGFA and AURKA gene up-regulation after MM-MMEC co-culture (**Supplementary Figure 3F, L)**.

These data support that MM-MMEC interactions enhance angiogenesis. Thus, we asked whether MM cells actively participate to the angiogenesis program in a reciprocal interaction with the BM microenvironment in patients and investigated if a pro-angiogenic gene-signature can detect patients with worse PFS and OS. Therefore, we interrogated 646 NDMM patients enrolled in the CoMMpass trial, comparing two different cohorts, based on survival outcome (alive *vs.* dead for OS and progressed *vs.* ongoing for PFS) performing a supervised analysis based on the gene expression of the pro-angiogenic factors contained in the angiogenesis array and other well-known JAM-A interactors. Strikingly, these two cohorts differed significantly: JAM-A, ENO-1, VEGFA and AURKA were all overexpressed in patients experiencing a shorter PFS and OS. Conversely, reduced TJP1 expression in patients correlated with poor survival (**Supplementary Table 3**). These gene expression data confirmed the protein expression results from our patient cohort. Exogenous JAM-A modulated the secretory profile of MMECs favoring angiogenesis and highlights the tight connection with an angiogenic environment, comprising key angiogenic factors, such as PLG, FGF-2, IGFBP1, VEGFA and VEGFC.

JAM-A inhibition impairs angiogenesis and inhibits tumor growth *in vivo*

To investigate whether JAM-A inhibition may affect *in vivo* angiogenesis and in turn MM-cell growth, we employed two different mouse models. To mimic advanced MM[21] we injected RPMI-8226 cells intratibially in NOD-SCID mice and analyzed bone specimens after α-JAM-A treatment.[2] Blocking JAM-A reduced MM cell proliferation and angiogenesis (**Figure 5A**). This difference

deemed statistically significant regarding numbers and percentage of Ki-67^{high} proliferating MM-cells (79.87 ± 1,242 and 35.38 ± 0,3455 in the ISO Control and in the α-JAM-A-treated group, respectively, *P*<.0001) and vessels/mm^2 field (9.3 and 7.1 in the ISO Control and in the α-JAM-A-treated group, respectively *P*<.0001) (**Figure 5B**). Also, the α-JAM-A treated group expressed lower JAM-A levels (79.78 ± 1,443 and 36.98 ± 0,466 in the ISO Control and in the α-JAM-A-treated group respectively *P*<.0001), lower CD31% (5.58 ± 1,34 and 3.48 ± 0,646 in the ISO Control and in the α-JAM-A-treated group, respectively *P*<.0001) and displayed a lower vessel density (calculated as vascular number/mm^2) than in the ISO Control, which presented a greater number of vessels with well-lit lumina (9.77 ± 2,63 and 6.48 ± 0,631 ISO Control *vs.* α-JAM-A-treated group, *P*<.0001).

To assess the activity of the anti-JAM-A blocking antibody on angiogenesis on a solitary plasmacytoma in vivo and to non-invasively monitor the MM cells growth at extraosseous sites with a caliper, we employed a subcutaneous MM xenograft model. This approach allows to dissect the endothelial bystander effect on BM-independent extramedullary MM.[21] Thus, we employed a second *in vivo* xenograft model engrafting RPMI-8226 cells s.c. into the flanks of NOD/SCID mice.[21] Animals were randomized at day three after engraftment and mice were treated either with α-JAM-A mAb or with a non-specific isotype control antibody i.p. for three days/week for 40 days. Subsequently, we measured the vascular area, the tumor volume and the hemoglobin content of the MM mass. Blocking α-JAM-A reduced the vascular area in the soft tissue MM masses in comparison to ISO Controls (difference between median -0.015, *P*<.0001). No adverse events occurred upon continuous α-JAM-A treatment.

Notably, after 40 days, the vascular area significantly increased in tumors and MM disease progressed more in controls compared to the α-JAM-A-treated group (**Figure 6A,** CD31 staining and **6B**). In ISO Control-treated mice, tumors grew exponentially contrasting only reduced tumor growth in α-JAM-A-treated animals (**Figure 6B and Supplementary Figure 4A)**. Lower hemoglobin content confirmed poor MM vascularization in the α-JAM-A-treated mice (8.4 ± 0.04 in ISO Control *vs.* 5.5 ± 0.04 in α-JAM-A-treated group, *P* <.0001, C.I. -3.02 to -2.8, **Figure 6C**). Ki-67-staining, vascular area and vessel count confirmed that blocking JAM-A strongly reduced the MM vascularity and disease progression. Furthermore, JAM-A blocking significantly reduced proangiogenic factors such as FGF-2 and VEGF-A in the peripheral blood plasma of MM bearing mice (**Supplementary Figure 4B-D)**.

Discussion

The angiogenic switch is a key process during transition from premalignant asymptomatic MGUS to full-blown MM. The evaluation of angiogenic parameters in the BM at the time of diagnosis was widely considered as a predictive factor for MM progression.[22] In solid tumors, such as breast, lung, head and neck and brain cancers, JAM-A activation promotes tumor

progression, while its inhibition by anti-JAM-A[2] agents reduces tumor growth.[11] We demonstrated in four independent experimental settings that JAM-A essentially stimulates MM-associated angiogenesis. In the CAM assay, a neutralizing α-JAM-A mAb caused strong reduction of the number of vessels, implying that JAM-A exerts an essential angiogenic *stimulus* that could not be replaced by any other compensating factor contained in the MMECs CM.[23] Our new findings pinpoint JAM-A as an attractive target in MM patients. JAM-A appears pivotal in MM evolution, which can be explained by several angiogenic mechanisms.[24,25] First, we demonstrated significantly increased JAM-A levels on MMECs from NDMM patients compared to MGECs. Furthermore, we could link the high JAM-A surface expression on MMECs with a significantly shorter OS in both ND- and RRMM and, at even more advanced disease stages, higher JAM-A expression levels correlated also with reduced PFS. Therefore, we examined the pathophysiologic basis responsible for favoring MM progression. As already described for HGF/cMET axis[26,27], JAM-A acts within the BM microenvironment, sustaining the neoplastic clone and promoting MM related angiogenesis both with direct and indirectly priming MMECs. Thus, JAM-A and its soluble isoform sJAM-A appear to feed into a vicious cycle involving the MMECs in generating a malignant environment favorable for MM progression. Although JAM-A is expressed in several solid cancers[3], to our knowledge this is the first report of endothelial JAM-A expression in its role for the MM tumor microenvironment. Homophilic interactions between recombinant sJAM-A and membrane JAM-A have been demonstrated biochemically.[10] Homophilic JAM-A interactions can be inhibited with an α-JAM-A mAb that binds to an epitope close to the N-terminus of the mature protein[10] as well as by a peptide that corresponds to the N-terminal 23 residues of the mature protein.[28] This suggests that the homophilic trans-interaction is mediated through the membrane-distal V-type Ig-like JAM-A domain at the N-terminus of the molecule. Targeting this domain of the JAM-A molecule on MMECs in our *in vitro* co-culture systems suggests that this type of interaction mediated the MM-MMEC crosstalk. In line with previous reports about MMECs sustaining MM growth[29,30], our disease models showed that during the transition from the pre- to the angiogenic phase, proliferation of tumor cells and neovascularization intensely involve over-expression of JAM-A on MMECs. MMECs were responsive to the presence of sJAM-A in the surrounding microenvironment, which increased their JAM-A surface protein expression. sJAM-A directly and indirectly upregulated JAM-A on the bystander MM-cells, independent from their basic JAM-A expression status. These observations support that cellular components of MM BM, including MMECs, can release JAM-A to sustain disease progression and prepare a tumor "friendly" niche, exerting significant modulation on FGF-2, VEGF-A and PLG/ENO1 downstream effect.

JAM-A has been described to interact with CD9, a well-known driver of MM-related drug resistance[31] and clinical prognosis.[32] We found a significant expression of FGF-2, a potent stabilizer and activator of a ternary complex involving JAM-A, CD9 and αvβ3 integrin, a novel

potential therapeutic target.[33] Peddibhotla *et al*. described that the aggregation of this ternary complex can activate downstream pathway cascades to induce proliferation, migration and an angiogenic *stimulus* to endothelial cells.[34] Our *in silico* validation shed more light on this pathophysiological process. ENO-1, encoding for the cytoplasmic α-Enolase, works as a plasminogen receptor and its up-regulated membrane expression is described in several cancer types.[35,36] Of note, plasminogen up-regulation had been correlated with tumor invasion and angiogenesis[37]; its activation, derived by the interaction with α-Enolase, prompted an activation of downstream signaling such as the MEK-ERK pathway, able to further promote cell invasion and angiogenesis. α-Enolase can also modulate the anti-tumor immune response. Cappello *et al*., described that α-Enolase^{high} myeloid-derived-suppressor-cells (MDSCs) could not adhere to TNFα primed endothelial cells in presence of an anti-ENO-1 mAb. Consequently, a decreased MDSC migration reduced the *in situ* immunosuppression enhancing the T cell-mediated immunity against malignant cells.[38,39]

We found that JAM-A overexpression in MMECs strongly correlated with ADAMTS1, a regulator of angiogenesis[40] and immune-surveillance[41], which appears to play a central role in preparing a favorable BM *milieu*.[42] We also identified that JAM-A surface expression on MMECs inversely correlated with ADAM17 expression. Conversely, sJAM-A release, directly correlated with ADAM17 upregulation, a mechanism described for endothelial cells in inflammation.[9] ADAM17 upregulation has been also observed in MM in the context of fractalkine release[43], which highlights this system as a potential novel therapeutic target in MM patients to disrupt a vicious circle formation enhancing the MM niche.

JAM-A also strongly correlated with AURKA in MM patients. This finding may link JAM-A mediated cell-adhesion to MM resilience and drug resistance.[20] Indeed, proteasome engulfment derived proteotoxicity[44] and invasiveness through epithelial-mesenchymal-transition and cell-adhesion[45] confer complex biological events that affect prognosis.[46] We also demonstrated that the interaction between MMECs and MM-cells affects JAM-A and other fundamental molecules, such as TJP1 and LFA-1 expression. This reciprocal "education" parallels the invasive attitude of the MM-cells towards the endothelial counterpart, instructing the vasculature to actively interact with the malignant cells, potentially driving their survival and drug resistance.[47,48] In line with this, increased JAM-A endothelial levels strongly correlated with unfavorable and resistant MM stages such as high R-ISS disease stages and the risk of extramedullary development.

An interaction network of JAM-A and α-Enolase[49] emphasizes the strong communication with the MM niche environment to allow persistence and sustaining proliferative signaling. Therefore, JAM-A may represent a key factor in the nurturing soil[50] to support MM evolution. Moschetta et *al*.[13] previously described the endothelium-MM-cells interdependency: EPCs trafficking enhances MM progression, particularly at an early disease stage. Rajkumar et *al*. highlighted a progressive increase in BM angiogenesis along the spectrum of plasma cell disorders from

MGUS to advanced MM.[12] Integrating the prognostic relevance of JAM-A expressed by MMECs and our experimental data prompts us to propose JAM-A as a key player in coordinating the interactions with the MM milieu enabling a permissive BM ecosystem during the aggressive disease evolution from NDMM to RRMM.

Indeed, the anti-MM effect of the JAM-A blocking also relies on its complex relationship with antiangiogenic effect, especially in critical transition phases of MM progression, such as the passage through MGUS to symptomatic MM and from responsive to drug-refractory disease, interfering with a main proangiogenic factor and with MM-cell proliferation. Our 2D and 3D models showed that mechanistically, JAM-A drives MM-associated angiogenesis via homophilic interaction and through identified downstream targets, namely FGF2, VEGF-A and PLG/ENO1, in the BM microenvironment. Moreover, the clinical impact demonstrated on a large cohort of consecutive individuals pinpoint JAM-A axis as a new player in the MM-associated angiogenesis able to better stratify patient's prognosis, especially in more advanced disease.

Collectively, the close link between MM and the BM microenvironment appears paradigmatic for MM evolution and disease progression. We connected the interaction of MMECs with MM-cells via the adhesion molecule JAM-A. Our data point towards a vicious cycle of JAM-A overexpression on MMECs mirrored in a higher JAM-A expression on the tumoral counterpart. Shed from the cell surface, sJAM-A enhances homophilic JAM-A complex establishment fostering MM niche formation. Finally, our results may open the development of JAM-A based therapeutic strategies directed against MM-interactions with the tumor microenvironment (**Figure 7A-D**). Clearly, these findings need to be confirmed in a larger patient population in a carefully designed prospective clinical study.

Acknowledgment

This work was supported by the Bayerische Forschungsstiftung consortium FortiTher (WP2TP3), the Deutsche Forschungsgemeinschaft μBone consortium (2084/1, 401253051), by the Italian Association for Cancer Research (AIRC) through an Investigator Grants (no. 20441 to VR), by the GLOBALDOC Project - CUP H96J17000160002 approved with A.D. n. 9 from Puglia Region, financed under the Action Plan for Cohesion approved with Commission decision C (2016) 1417 to AGS. This research project was supported in part by the Apulian Regional Project "Medicina di Precisione" to AGS. AR was supported by the Wilhelm Sander-Stiftung (Grant no. 2014.903.1). The authors acknowledge the Multiple Myeloma Research Foundation for providing an updated and comprehensive real-life MM dataset for the international scientific community. The *in silico* analysis and the relative clinical correlation were generated as part of the Multiple Myeloma Research Foundation Personalized Medicine Initiative.

We thank the members of the Beilhack and Vacca labs for vivid discussions. We also thank Drs. Julia Delgado Tascón, Claudia Siverino, Marco Metzger and Mss Katharina Schmiedgen, Charlotte Botz-Von Drathen, Hannah Manz and Vittoria Musci for technical support and valuable discussions.

Contribution: AGS, MCDV, VR, HE, AV and AB designed and performed research, analyzed and interpreted data and wrote the manuscript; AGS, MCDV, PL, GC, PTG, GDL, ABra, EH, HR-W, DR performed research and analyzed data; AGS, MCDV, AA, PB, GC, FPB, AM, SDS, TS, ABal, MAF, WK, AR and ST analyzed data; AGS, HE, RR, LR, PD, KMK, VR and AV provided patient samples; AGS, MCDV, CT, MC, VR, AV, HE and AB designed research, interpreted data, and edited the manuscript; all authors revised the manuscript and approved submission.

Public consulted datasets are available at https://research.mmrf.org, CoMMpass longitudinal, prospective observational study (release IA12).

Disclosure of conflicts of interest

The authors declare no conflict of interest.

References

1. Steinbacher T, Kummer D, Ebnet K. Junctional adhesion molecule-A: functional diversity through molecular promiscuity. Cell Mol Life Sci. 2018;75(8):1393-1409.
2. Solimando AG, Brandl A, Mattenheimer K, et al. JAM-A as a prognostic factor and new therapeutic target in multiple myeloma. Leukemia. 2018;32(3):736-743.
3. Leech AO, Cruz RGB, Hill ADK, Hopkins AM. Paradigms lost-an emerging role for over-expression of tight junction adhesion proteins in cancer pathogenesis. Ann Transl Med. 2015;3(13):184.
4. Severson EA, Parkos CA. Mechanisms of outside-in signaling at the tight junction by junctional adhesion molecule A. Ann N Y Acad Sci. 2009;1165:10-18.
5. Ebnet K, Schulz CU, Meyer Zu Brickwedde MK, Pendl GG, Vestweber D. Junctional adhesion molecule interacts with the PDZ domain-containing proteins AF-6 and ZO-1. J Biol Chem. 2000;275(36):27979-27988.
6. Ebnet K. Junctional Adhesion Molecules (JAMs): Cell Adhesion Receptors With Pleiotropic Functions in Cell Physiology and Development. Physiol Rev. 2017;97(4):1529-1554.
7. Terral G, Champion T, Debaene F, et al. Epitope characterization of anti-JAM-A antibodies using orthogonal mass spectrometry and surface plasmon resonance approaches. mAbs. 2017;9(8):1317-1326.
8. Vellanki SH, Cruz RGB, Jahns H, et al. Natural compound Tetrocarcin-A downregulates Junctional Adhesion Molecule-A in conjunction with HER2 and inhibitor of apoptosis proteins and inhibits tumor cell growth. Cancer Lett. 2019;440-441:23-34.
9. Koenen RR, Pruessmeyer J, Soehnlein O, et al. Regulated release and functional modulation of junctional adhesion molecule A by disintegrin metalloproteinases. Blood. 2009;113(19):4799-4809.
10. Bazzoni G, Martinez-Estrada OM, Orsenigo F, Cordenonsi M, Citi S, Dejana E. Interaction of junctional adhesion molecule with the tight junction components ZO-1, cingulin, and occludin. J Biol Chem. 2000;275(27):20520-20526.
11. Murakami M, Francavilla C, Torselli I, et al. Inactivation of junctional adhesion molecule-A enhances antitumoral immune response by promoting dendritic cell and T lymphocyte infiltration. Cancer Res. 2010;70(5):1759-1765.
12. Rajkumar SV, Mesa RA, Fonseca R, et al. Bone marrow angiogenesis in 400 patients with monoclonal gammopathy of undetermined significance, multiple myeloma, and primary amyloidosis. Clin Cancer Res. 2002;8(7):2210-2216.
13. Moschetta M, Mishima Y, Kawano Y, et al. Targeting vasculogenesis to prevent progression in multiple myeloma. Leukemia. 2016;30(5):1103-1115.
14. Rajkumar SV, Dimopoulos MA, Palumbo A, et al. International Myeloma Working Group updated criteria for the diagnosis of multiple myeloma. Lancet Oncol. 2014;15(12):e538-548.
15. Rajkumar SV, Harousseau J-L, Durie B, et al. Consensus recommendations for the uniform reporting of clinical trials: report of the International Myeloma Workshop Consensus Panel 1. Blood. 2011;117(18):4691-4695.
16. Rao L, De Veirman K, Giannico D, et al. Targeting angiogenesis in multiple myeloma by the VEGF and HGF blocking DARPin® protein MP0250: a preclinical study. Oncotarget. 2018;9(17):13366-13381.
17. Jridi I, Catacchio I, Majdoub H, et al. The small subunit of Hemilipin2, a new heterodimeric phospholipase A2 from Hemiscorpius lepturus scorpion venom, mediates the antiangiogenic effect of the whole protein. Toxicon. 2017;126:38-46.
18. Nowak-Sliwinska P, Alitalo K, Allen E, et al. Consensus guidelines for the use and interpretation of angiogenesis assays. Angiogenesis. 2018;21(3):425-532.
19. Ribatti D, Nico B, Vacca A, Presta M. The gelatin sponge-chorioallantoic membrane assay. Nat Protoc. 2006;1(1):85-91.
20. Qin Y, Zhang S, Deng S, et al. Epigenetic silencing of miR-137 induces drug resistance and chromosomal instability by targeting AURKA in multiple myeloma. Leukemia. 2017;31(5):1123-1135.
21. Mitsiades CS, Anderson KC, Carrasco DR. Mouse models of human myeloma. Hematol

Oncol Clin North Am. 2007;21(6):1051-1069, viii.
22. Rajkumar SV, Leong T, Roche PC, et al. Prognostic value of bone marrow angiogenesis in multiple myeloma. Clin Cancer Res. 2000;6(8):3111-3116.
23. Ria R, Catacchio I, Berardi S, et al. HIF-1α of bone marrow endothelial cells implies relapse and drug resistance in patients with multiple myeloma and may act as a therapeutic target. Clin Cancer Res. 2014;20(4):847-858.
24. Fukuhara T, Kim J, Hokaiwado S, et al. A novel immunotoxin reveals a new role for CD321 in endothelial cells. PloS One. 2017;12(10):e0181502.
25. Stamatovic SM, Sladojevic N, Keep RF, Andjelkovic AV. Relocalization of junctional adhesion molecule A during inflammatory stimulation of brain endothelial cells. Mol Cell Biol. 2012;32(17):3414-3427.
26. Moschetta M, Basile A, Ferrucci A, et al. Novel targeting of phospho-cMET overcomes drug resistance and induces antitumor activity in multiple myeloma. Clin Cancer Res. 2013;19(16):4371-4382.
27. Ferrucci A, Moschetta M, Frassanito MA, et al. A HGF/cMET autocrine loop is operative in multiple myeloma bone marrow endothelial cells and may represent a novel therapeutic target. Clin Cancer Res. 2014;20(22):5796-5807.
28. Babinska A, Kedees MH, Athar H, et al. F11-receptor (F11R/JAM) mediates platelet adhesion to endothelial cells: role in inflammatory thrombosis. Thromb Haemost. 2002;88(5):843-850.
29. Cooke VG, Naik MU, Naik UP. Fibroblast growth factor-2 failed to induce angiogenesis in junctional adhesion molecule-A-deficient mice. Arterioscler Thromb Vasc Biol. 2006;26(9):2005-2011.
30. Leone P, Di Lernia G, Solimando AG, et al. Bone marrow endothelial cells sustain a tumor-specific CD8+ T cell subset with suppressive function in myeloma patients. Oncoimmunology. 2019;8(1):e1486949.
31. Hu X, Xuan H, Du H, Jiang H, Huang J. Down-regulation of CD9 by methylation decreased bortezomib sensitivity in multiple myeloma. PloS One. 2014;9(5):e95765.
32. De Bruyne E, Bos TJ, Asosingh K, et al. Epigenetic silencing of the tetraspanin CD9 during disease progression in multiple myeloma cells and correlation with survival. Clin Cancer Res. 2008;14(10):2918-2926.
33. Wallstabe L, Mades A, Frenz S, Einsele H, Rader C, Hudecek M. CAR T cells targeting αvβ3 integrin are effective against advanced cancer in preclinical models. Adv Cell Gene Ther. 2018;1(2):e11.
34. Peddibhotla SSD, Brinkmann BF, Kummer D, et al. Tetraspanin CD9 links junctional adhesion molecule-A to αvβ3 integrin to mediate basic fibroblast growth factor-specific angiogenic signaling. Mol Biol Cell. 2013;24(7):933-944.
35. Tu S-H, Chang C-C, Chen C-S, et al. Increased expression of enolase alpha in human breast cancer confers tamoxifen resistance in human breast cancer cells. Breast Cancer Res Treat. 2010;121(3):539-553.
36. Yu Y-Q, Wang L, Jin Y, et al. Identification of serologic biomarkers for predicting microvascular invasion in hepatocellular carcinoma. Oncotarget. 2016;7(13):16362-16371.
37. Rossignol P, Ho-Tin-Noé B, Vranckx R, et al. Protease nexin-1 inhibits plasminogen activation-induced apoptosis of adherent cells. J Biol Chem. 2004;279(11):10346-10356.
38. Cappello P, Tonoli E, Curto R, Giordano D, Giovarelli M, Novelli F. Anti-α-enolase antibody limits the invasion of myeloid-derived suppressor cells and attenuates their restraining effector T cell response. Oncoimmunology. 2016;5(5):e1112940.
39. Castella B, Foglietta M, Riganti C, Massaia M. Vγ9Vδ2 T Cells in the Bone Marrow of Myeloma Patients: A Paradigm of Microenvironment-Induced Immune Suppression. Front Immunol. 2018;9:1492.
40. Casal C, Torres-Collado AX, Plaza-Calonge MDC, et al. ADAMTS1 contributes to the acquisition of an endothelial-like phenotype in plastic tumor cells. Cancer Res. 2010;70(11):4676-4686.
41. Hope C, Foulcer S, Jagodinsky J, et al. Immunoregulatory roles of versican proteolysis in the myeloma microenvironment. Blood. 2016;128(5):680-685.
42. Li J, Zou K, Yu L, et al. MicroRNA-140 Inhibits the Epithelial-Mesenchymal Transition and

Metastasis in Colorectal Cancer. Mol Ther Nucleic Acids. 2018;10:426-437.
43. Marchica V, Toscani D, Corcione A, et al. Bone Marrow CX3CL1/Fractalkine is a New Player of the Pro-Angiogenic Microenvironment in Multiple Myeloma Patients. Cancers. 2019;11(3):321.
44. Savitski MM, Zinn N, Faelth-Savitski M, et al. Multiplexed Proteome Dynamics Profiling Reveals Mechanisms Controlling Protein Homeostasis. Cell. 2018;173(1):260-274.e25.
45. Ren B-J, Zhou Z-W, Zhu D-J, et al. Alisertib Induces Cell Cycle Arrest, Apoptosis, Autophagy and Suppresses EMT in HT29 and Caco-2 Cells. Int J Mol Sci. 2015;17(1):41.
46. Noll JE, Vandyke K, Hewett DR, et al. PTTG1 expression is associated with hyperproliferative disease and poor prognosis in multiple myeloma. J Hematol Oncol. 2015;8:106.
47. Waldschmidt JM, Simon A, Wider D, et al. CXCL12 and CXCR7 are relevant targets to reverse cell adhesion-mediated drug resistance in multiple myeloma. Br J Haematol. 2017;179(1):36-49.
48. Zhang X-D, Baladandayuthapani V, Lin H, et al. Tight Junction Protein 1 Modulates Proteasome Capacity and Proteasome Inhibitor Sensitivity in Multiple Myeloma via EGFR/JAK1/STAT3 Signaling. Cancer Cell. 2016;29(5):639-652.
49. Ramroop JR, Stein MN, Drake JM. Impact of Phosphoproteomics in the Era of Precision Medicine for Prostate Cancer. Front Oncol. 2018;8:28.
50. Mundy GR. Metastasis to bone: causes, consequences and therapeutic opportunities. Nat Rev Cancer. 2002;2(8):584-593.

Figure legends

Figure 1. Elevated JAM-A expression on BM primary MM endothelial cells (MMECs) in newly diagnosed patients (NDMM) correlates with poor OS. (**A**) Relative mRNA expression level of JAM-A of MMECs compared to MGECs by RT real time-PCR (n=73 MGUS patients derived MGECs and 73 NDMM derived MMECs), **** *P*< 0.0001, Mann-Whitney test. (**B**) Western Blot densitometric analysis of basal protein expression of JAM-A of MGECs and MMECs lysates normalized to β-actin (n=24 MGUS patients derived MGECs and 24 NDMM derived MMECs). Results are presented as mean ± SD, **** *P*< 0.0001, Mann-Whitney test. (**C**) FACS analysis of JAM-A cell surface expression from representative patient-derived MMECs, identified as CD45/138/38^{neg}/31^{pos} cells. **(D)** JAM-A overexpression colocalizes with a higher vessel density on bone marrow biopsies. Vessel density (as highlighted by CD34 [red] staining) was higher in bone marrow spaces infiltrated by JAM-A^{high} (brown) neoplastic plasma cells, as compared to JAM-A^{low} cases. Magnification x 200. Scale bar=50 μm **(E)** Kaplan-Meier estimator of OS, by level of surface MMECs JAM-A expression. The median OS estimated in subjects with JAM-A^{low} MMECs cells at FACS was not reached whereas in subjects with JAM-A^{high} MMECs the median OS was 78 months (HR= 9.14, 95% CI 2.8–29.76, *P*< 0.0001; χ^2_{LR}=20.11; *P*< 0.0001, upper panel). Uni- and multivariate analysis (lower panel). BM: bone marrow; MGECs: MGUS derived endothelial cells; NDMM: newly diagnosed MM; Pts: patients. OS: overall survival; NR: not reached. R-ISS: Revised International Staging System; Hb: hemoglobin.

Figure 2. **Elevated JAM-A expression on bone marrow primary MM endothelial cells (MMECs) predicts poor prognosis in relapsed refractory multiple myeloma (RRMM).** Kaplan-Meier estimator of OS (**A**) and PFS (**B**), by level of surface MMECs JAM-A expression. (**C**) Cox model - set on OS and PFS analyses. The median follow-up was 53 months (4–262 months) for OS and 23 months (1–119 months) for PFS. *Cox models adjusted for sex and age. **Cox stratified hazards regression by chronic kidney disease. OS: overall survival; PFS: progression free

survival; MMECs: bone marrow primary MM endothelial cells. Pts: patients. NR: not reached. R-ISS: Revised International Staging System; Hb: hemoglobin.

Figure 3. BM primary MM endothelial cells (MMECs) enhance JAM-A expression on MM-cells. Experimental designs depicted at the top. RPMI-8226 cells have been cultured alone or co-cultured with MMECs at 1:5 ratio (RPMI-8266:MMECs) in inserted transwells and analyzed for JAM-A expression with Western blot (**A**) and flow cytometry (**B**). (**C**) RPMI-8226 cells were maintained for 24 hours in conditioned media from MMECs or MGECs. Cells were harvested and lysed and the extracted proteins immunoblotted for JAM-A expression. Overall densitometric analyses are reported. (**D**) RPMI-8226 cells were also analyzed at FACS after culture for 24 hours in MGECs or MMECs CM. Results are presented as mean ± SD, (n=24 MGUS patients derived MGECs and 24 NDMM derived MMECs), *P*< 0.0001 ****, Mann-Whitney test. BM: bone marrow; MGECs: MGUS derived endothelial cells; NDMM: newly diagnosed MM; CM: conditioned medium; MFI: mean fluorescence intensity.

Figure 4. Pivotal role of JAM-A in MM associated angiogenesis in 2D and 3D conditions. (**A**) Upper panel. Confluent monolayers of MMECs underwent a *scratch wound-healing* assay. 3 hours after scratching photographs were taken of MMECs that had been maintained in MMECs CM alone (CTRL) or previously supplemented for 12 hours with sJAM-A at 100 ng/mL and added isotype control (+sJAM-A +ISO) or α-JAM-A (+sJAM-A +α-JAM-A) blocking antibody. Lower panel: Migrating cells in each wound were counted. Counts of proliferating and migrating cells of six independent experiments. **** *P*< 0.0001, Mann-Whitney test. (**B**) Photographs at 3 hours of newly-formed capillary networks after MMECs were seeded on Matrigel™ layer. Direct comparison of MMECs in CM *vs*. MMECs treated with 100 ng/ml sJAM-A (upper left panel). Independent experiment to assess JAM-A inhibition in MMECs either treated with an anti-JAM-A blocking antibody *vs*. isotype control antibody (upper right panel). Independent experiment to assess JAM-A knock-down in MMECs comparing treatment with JAM-A specific siRNA *vs*. non-specific scrambled siRNA without addition of sJAM-A (lower left panel). Independent experiment to assess

the effect of blocking JAM-A after addition 100 ng/ml of sJAM-A by comparing capillary formation after MMECs treatment with sJAM-A and anti-JAM-A blocking antibody *vs*. sJAM-A and isotype control antibody (lower right quadrant). Representative pictures of three biological replicates. Skeletonization of the meshes were analyzed and branching points measured. Data are normalized to control. Scale bar=100 μm. (**C**) Chorioallantoic membrane assay with the gelatin sponge loaded with MMECs CM alone (CTRL) or with MMECs CM supplemented with sJAM-A (+sJAM-A), in presence or absence of 0,5 μg/ml α-JAM-A mAb. On day 12, pictures were taken *in ovo*. One representative experiment is shown at 50X magnification. Newly formed vessels were counted. Mann-Whitney test. (**D**) An array of 55 human angiogenesis related proteins was performed on MMECs CM after sJAM-A treatment without and with blocking with the α-JAM-A mAb. Array spots were analyzed with ImageJ Lab v. 1.51 software and normalized to positive control signal intensities. Graph bars represent the pixel density of the detected angiogenesis-related cytokines in two independent experiments. Values are expressed as mean ± SD of ten independent experiments. Mann-Whitney test. * $P< 0.05$; and **** $P< 0.0001$, versus SFM as control. See **Supplementary Figure 3** and the main text for more details. MMECs: bone marrow primary MM endothelial cells; CM: conditioned medium; CTRL: control; SFM: serum free medium; n.s.= not significant. CAM: Chick chorioallantoic membrane.

Figure 5. JAM-A inhibition reduces MM proliferation and vasculature in intratibial MM *in vivo* model. NOD/SCID mice (n= 20) bearing RPMI-8226 intratibial xenograft were repetitiously treated with α-JAM-A blocking mAb, or isotope control IgG (ISO) for three weeks. (**A**) Upper panel. From left to the right. Ki67/CD138 and JAM-A staining: CD138 and JAM-A (red) reactivity appears to be more represented on the smaller neoplastic plasma cells, whereas the most pleomorphic/anaplastic component shows lower reactivity; a reverse staining distribution is observed for Ki67 nuclear staining (brown), which is more prominent on the larger cells. CD31/JAM-A double and CD31 coloration (brown) highlights endothelia lining thin walled microvessels; lumina appear to be only slightly dilated; JAM-A (red) stains a fraction of neoplastic plasma cells, with a cytoplasmic pattern. Lower panel. Decreased Ki67 expression in α-JAM-A

derived specimen. Within the CD31 stained noninvolved BM lacunae (see $CD31^+$ megakaryocytes) from the α-JAM-A treated group the vessels are more distended, and endothelia display a thin, inconspicuous cytoplasmic rim. (**B**) From left to the right, differences in terms of MM proliferation, JAM-A, CD31 positivity on endothelial cells and vessels count, assessed by two pathologists. Data shown are mean ± SD from ten individual mice for each group. **** *P*< .0001 versus controls, obtained with Mann-Whitney test. Scale bar=100 μm. BM: bone marrow.

Figure 6. JAM-A inhibition restricts angiogenesis and tumor growth in subcutaneous MM xenograft model. NOD/SCID mice (n= 20) bearing RPMI-8226 subcutaneous xenograft were repetitiously treated with α-JAM-A blocking mAb, or isotope control IgG (ISO) or with vehicle only for 40 days for 3 days/week. (**A**) Immunohistochemistry staining: JAM-A (red) reactivity is higher in the smaller neoplastic cells whereas in most pleomorphic/anaplastic components it is lower. A reverse staining distribution is observed for Ki67 nuclear staining (brown), which is more clear-cut in the larger cells. CD31 staining shows focal positivity in the control group and it is absent in the α-JAM-A group. (**B**) Treatment was continued for three days a week for 40 days and tumor volumes were measured every two days with a caliper. (**C**) Hemoglobin values, Ki-67 positivity, vessel area and number of vessels expressed as mean ± SD of three independent experiments. **P*< 0.05 versus vehicle-treated control. Scale bar=50 μm.****P*< .0001 versus controls obtained with Mann-Whitney test.

Figure 7. **JAM-A boosts MM-related angiogenesis in the BM microenvironment. (A)** Molecular interactions between MM-cells and MMECs: cell-adhesion mediated changes via trans-homo/heterophilic JAM-A interaction. **(B)** FGF-2 mediates pro-angiogenic and proliferative role of JAM-A and its release as monomeric JAM-A from the ternary complex through an unknown mechanism. We speculate that once monomeric JAM-A is available at a membrane level, it forms homodimers that mediate downstream signaling and is also susceptible for cleavage and shedding via ADAM17. **(C)** JAM-A mediated cytoskeleton rearrangement via TJP1 down regulation and cell function modification: depending on myeloma cells-mediated interactions the endothelial cells can lose their tight junction and be prone to increase the vascular permeability. **(D)** PLG/ENO1

interaction triggers angiogenesis and microenvironment modification via JAM-A. Caveolin1 modulates the transport of cytosolic ENO-1 to the cell surface. BM: bone marrow; MMECs: bone marrow primary MM endothelial cells; FGF-2: Fibroblast growth factor-2; ADAM17: ADAM metallopeptidase domain 17; TJP1: Tight junction protein-1; PLG: plasminogen; ENO1: Enolase 1; LFA-1: Lymphocyte function-associated antigen 1; MAPK: mitogen-activated protein kinase; $\alpha V\beta 3$: Integrin alpha V beta 3; CD9: CD9 Molecule; VEGFA: Vascular Endothelial Growth Factor A; ADAMTS1: Human Metalloproteinase with Thrombospondin Type 1 Motifs. AURKA: Aurora Kinase A. See results and discussion for additional details.

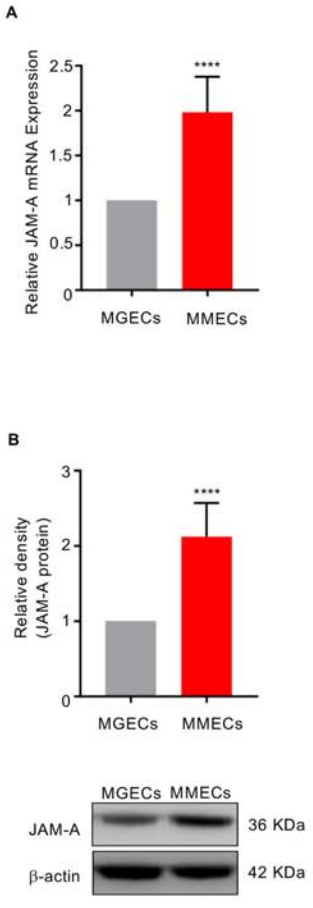

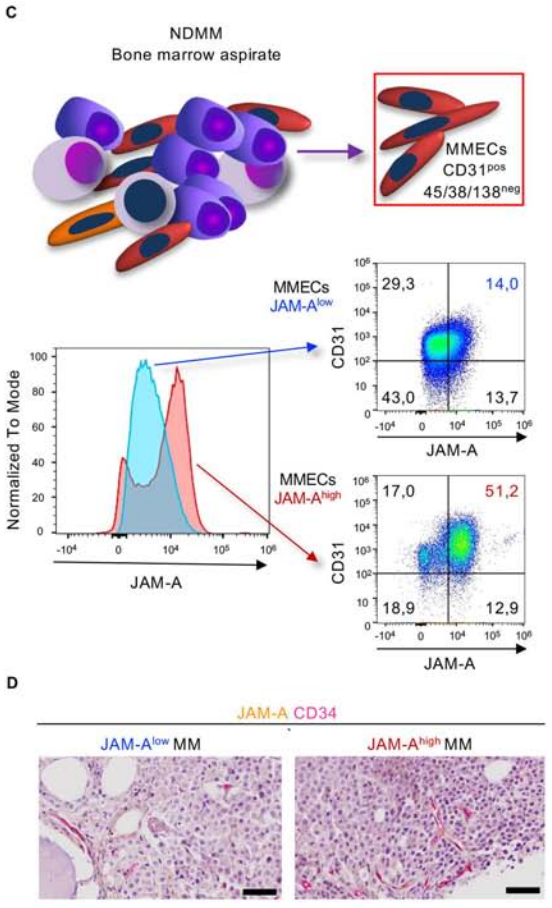

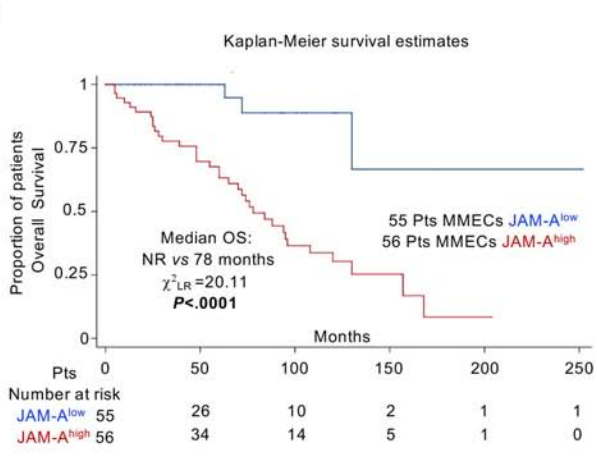

	*Cox model for Overall Survival			
	Univariate analysis		Multivariate analysis	
	HR (95%CI)	*P* value	HR (95%CI)	*P* value
MMECs JAM-A surface expression (JAM-A^{high} vs JAM-A^{low})	9.14 (2.80-29.76)	**<0.001**	9.11 (2.79-29.76)	**<0.001**
Bone Lesion (Yes vs No)	1.31 (0.60-2.89)	0.489	-	-
Hb (<10 vs >/-10 g/dL)	1.44 (0.75-2.77)	0.271	-	-
R-ISS **R-Stage I** **R-Stage II** **R-Stage III**	 1 1.37 (0.55-3.39) 2.11 (0.76-5.86)	 0.494 0.149	-	-
Sex (M vs F)	0.58 (0.29-1.13)	0.110	0.65 (0.33-1.30)	0.233
Chronic kidney disease (Yes vs No)	2.04 (1.05-3.96)	**0.033**	2.11 (1.08-4.10)	**0.027**
Age	0.98 (0.94-1.02)	0.542	0.99 (0.95-1.04)	0.984

Figure 1

A

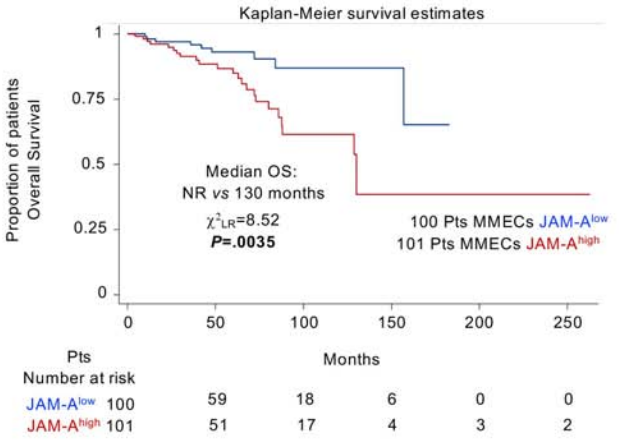

B

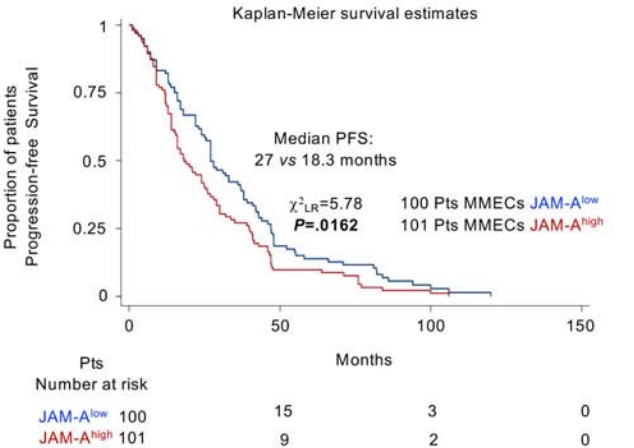

C

	*Cox model for Overall Survival				*Cox model for Progression-Free Survival			
	Univariate analysis		Multivariate analysis		Univariate analysis		**Multivariate analysis	
	HR (95%CI)	*P* value	HR (95%CI)	*P* value	HR (95%CI)	*P* value	HR (95%CI)	*P* value
MMECs JAM-A surface expression (JAM-A^{high} vs JAM-A^{low})	2.96 (1.37-6.37)	**0.006**	2.39 (1.09-5.28)	**0.030**	1.41 (1.05-1.88)	**0.019**	1.35 (1.00-1.81)	**0.044**
Bone Lesion (Yes vs No)	1.57 (0.72-3.40)	0.247	-	-	1.09 (0.81-1.48)	0.546	-	-
Hb level (<10 vs >/-10 Hb/dl)	3.19 (1.60-6.34)	**0.001**	-	-	1.35 (0.98-1.86)	0.063	-	-
R-ISS								
R-Stage I	1		1		1		1	
R-Stage II	7.20 (1.70-30.39)	**0.007**	5.34 (1.24-22.97)	**0.024**	1.05 (0.77-1.45)	0.727	0.96 (0.68-1.33)	0.814
R-Stage III	8.58 (1.66-44.35)	**0.010**	6.57 (1.25-34.54)	**0.026**	0.98 (0.57-1.67)	0.953	0.95 (0.55-1.64)	0.866
Sex (M vs F)	1.49 (0.73-3.05)	0.272	1.28 (0.59-2.78)	0.520	1.04 (0.77-1.40)	0.780	1.06 (0.78-1.45)	0.669
Chronic kidney disease (Yes vs No)	2.43 (1.22-4.83)	**0.011**	2.12 (1.00-4.52)	**0.049**	1.54 (1.13-2.11)	**0.006**	-	-
Age	1.01 (0.98-1.05)	0.407	1.01 (0.97-1.05)	0.428	1.00 (0.99-1.02)	0.342	0.99 (0.98-1.01)	0.877

Figure 2

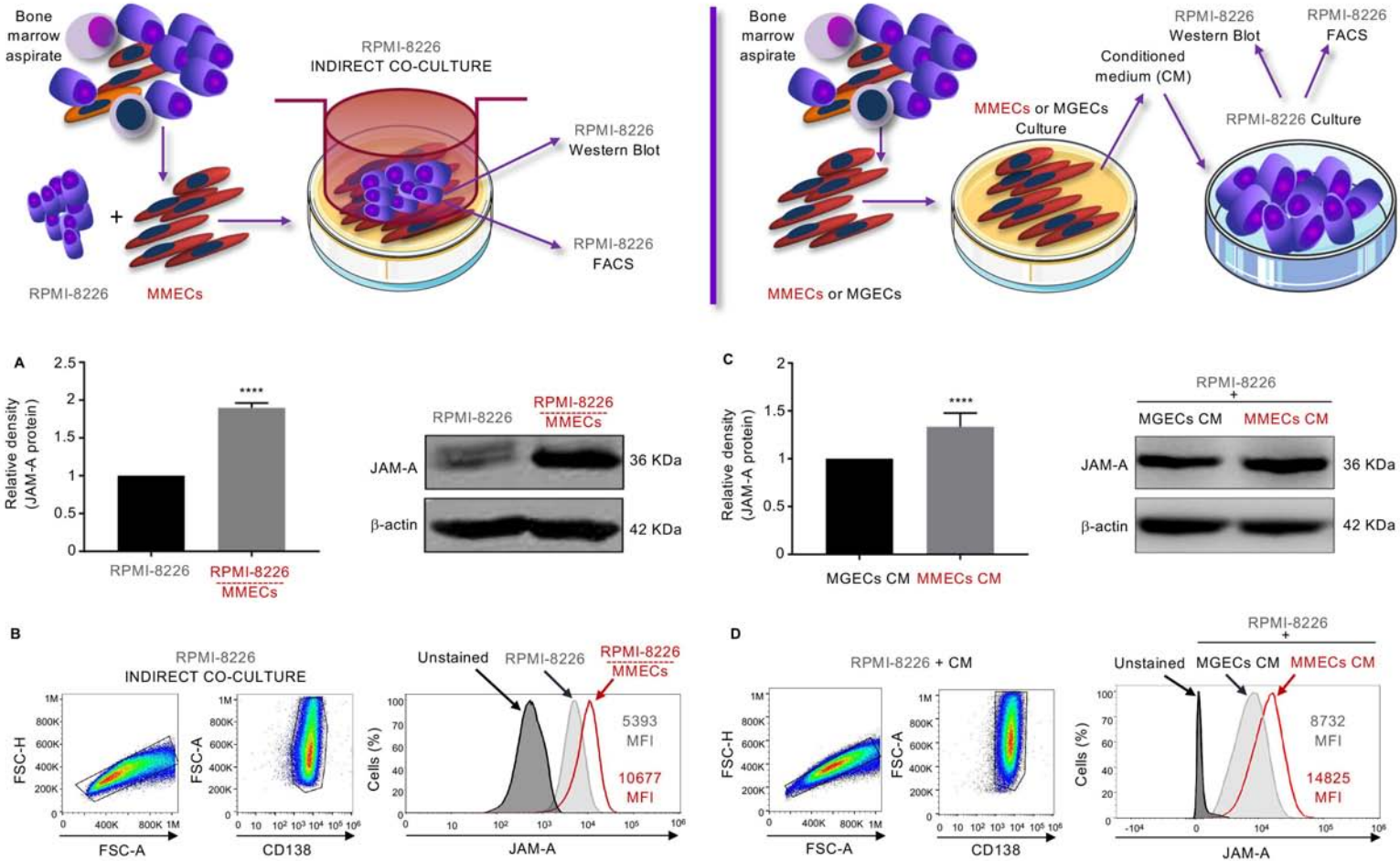
Bone marrow aspirate
RPMI-8226
MMECs
RPMI-8226
INDIRECT CO-CULTURE
RPMI-8226 Western Blot
RPMI-8226 FACS
Bone marrow aspirate
MMECs or MGECs
MMECs or MGECs Culture
Conditioned medium (CM)
RPMI-8226 Western Blot
RPMI-8226 FACS
RPMI-8226 Culture
A
Relative density (JAM-A protein)
****
RPMI-8226
RPMI-8226 MMECs
RPMI-8226
RPMI-8226 MMECs
JAM-A
36 KDa
β-actin
42 KDa
C
Relative density (JAM-A protein)
****
MGECs CM
MMECs CM
RPMI-8226 +
MGECs CM
MMECs CM
JAM-A
36 KDa
β-actin
42 KDa
B
RPMI-8226
INDIRECT CO-CULTURE
FSC-H
FSC-A
FSC-A
CD138
Unstained
RPMI-8226
RPMI-8226 MMECs
5393 MFI
10677 MFI
Cells (%)
JAM-A
D
RPMI-8226 + CM
FSC-H
FSC-A
FSC-A
CD138
RPMI-8226 +
Unstained
MGECs CM
MMECs CM
8732 MFI
14825 MFI
Cells (%)
JAM-A

Figure 3

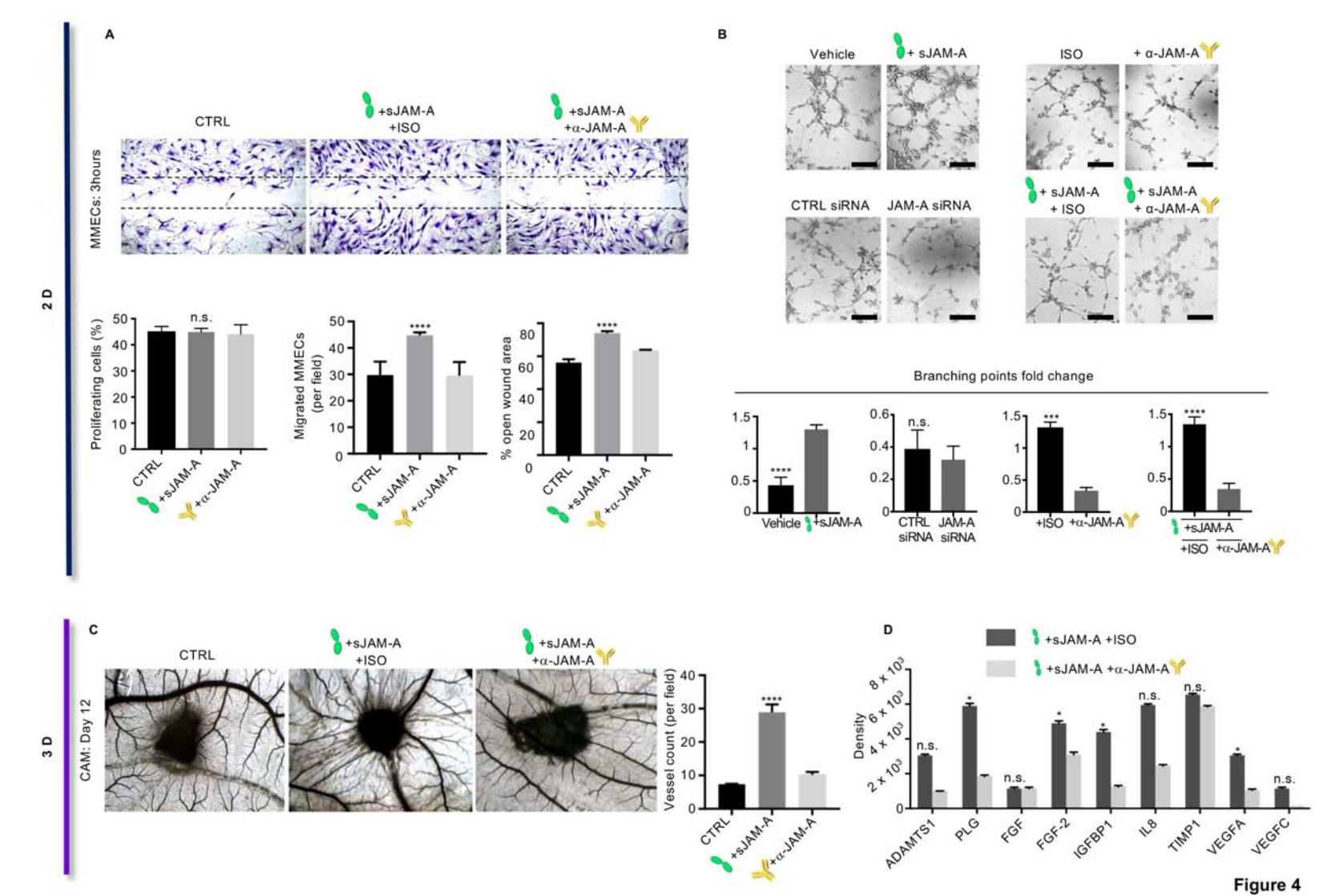
2 D
3 D
A
CTRL
+sJAM-A +ISO
+sJAM-A +α-JAM-A
MMECs: 3hours
Proliferating cells (%)
n.s.
Migrated MMECs (per field)
****
% open wound area
****
CTRL
+sJAM-A
+α-JAM-A
B
Vehicle
+ sJAM-A
ISO
+ α-JAM-A
CTRL siRNA
JAM-A siRNA
+ sJAM-A + ISO
+ sJAM-A + α-JAM-A
Branching points fold change
****
n.s.
***
****
Vehicle
+sJAM-A
CTRL siRNA
JAM-A siRNA
+ISO
+α-JAM-A
C
CAM: Day 12
CTRL
+sJAM-A +ISO
+sJAM-A +α-JAM-A
Vessel count (per field)
****
D
+sJAM-A +ISO
+sJAM-A +α-JAM-A
Density
n.s.
*
n.s.
*
*
n.s.
n.s.
*
n.s.
ADAMTS1
PLG
FGF
FGF-2
IGFBP1
IL8
TIMP1
VEGFA
VEGFC

Figure 4

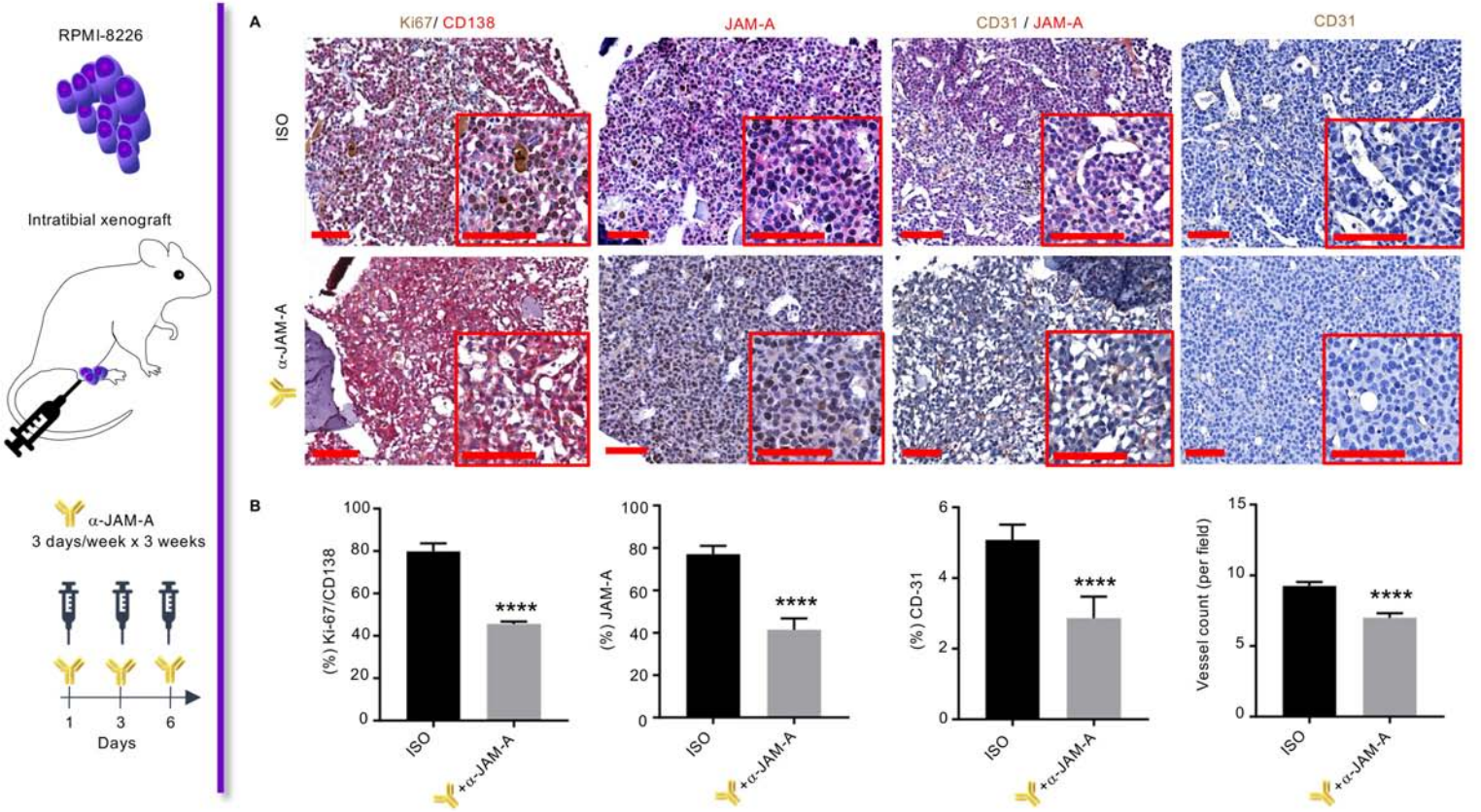
RPMI-8226
Intratibial xenograft
α-JAM-A
3 days/week x 3 weeks
1
3
6
Days
A
Ki67/ CD138
JAM-A
CD31 / JAM-A
CD31
ISO
α-JAM-A
B
(%) Ki-67/CD138
(%) JAM-A
(%) CD-31
Vessel count (per field)
****
ISO
+α-JAM-A

Figure 5

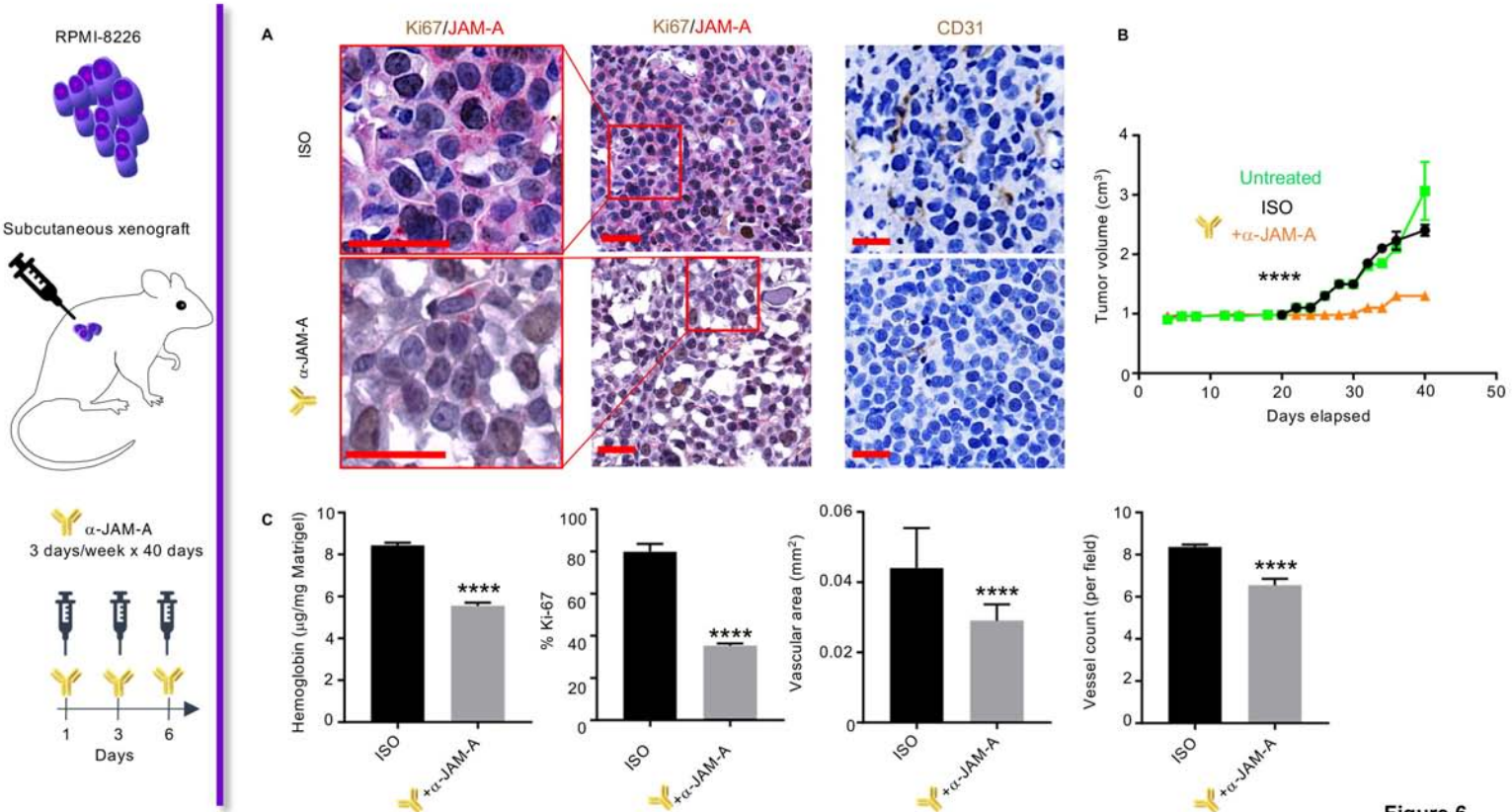
RPMI-8226
Subcutaneous xenograft
α-JAM-A
3 days/week x 40 days
1
3
6
Days
A
Ki67/JAM-A
Ki67/JAM-A
CD31
ISO
α-JAM-A
B
Untreated
ISO
+α-JAM-A
****
Tumor volume (cm³)
Days elapsed
C
Hemoglobin (μg/mg Matrigel)
% Ki-67
Vascular area (mm²)
Vessel count (per field)
****
ISO
+α-JAM-A

Figure 6

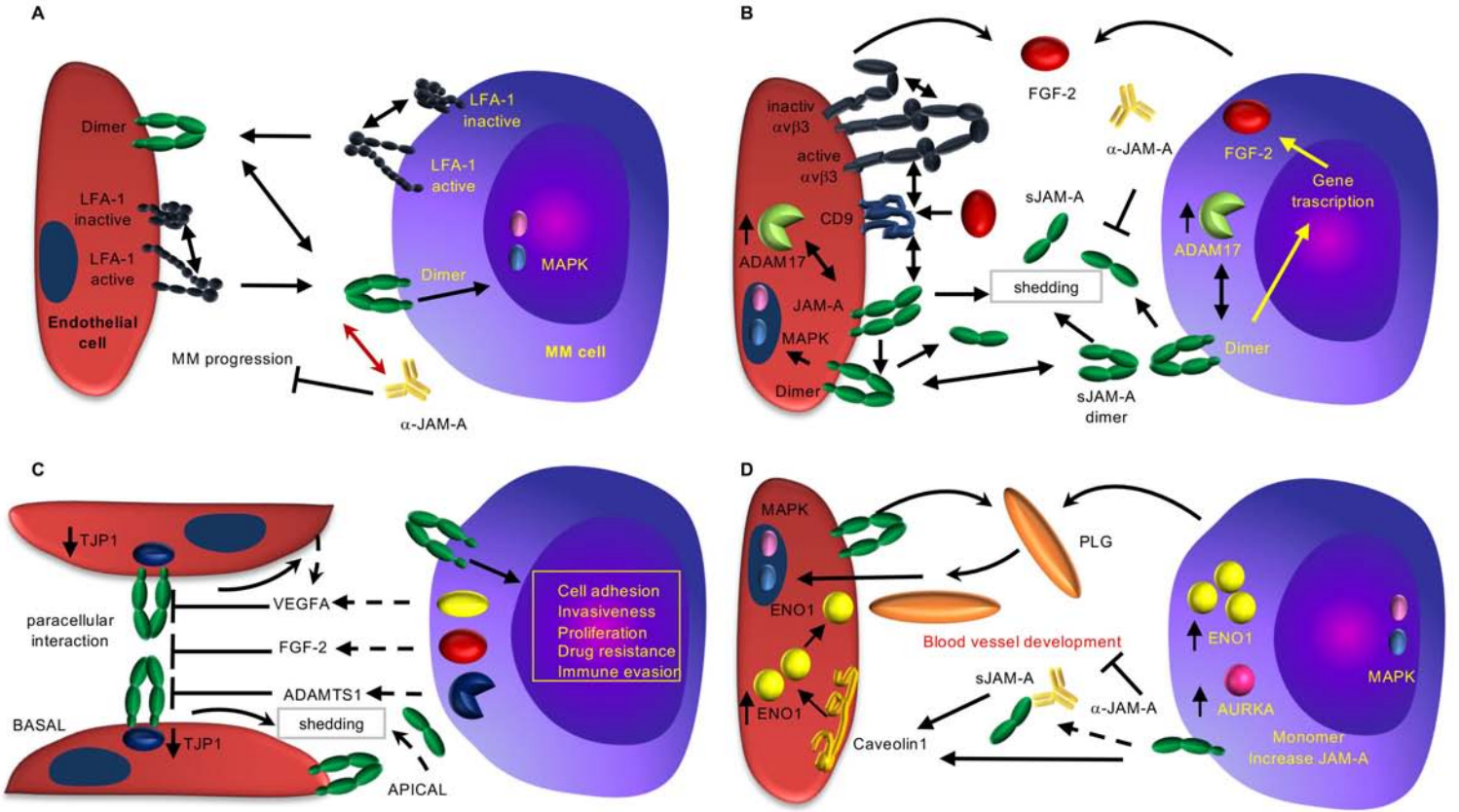
A
Dimer
LFA-1 inactive
LFA-1 active
Endothelial cell
LFA-1 inactive
LFA-1 active
Dimer
MAPK
MM cell
MM progression
α-JAM-A
B
inactiv αvβ3
active αvβ3
CD9
ADAM17
JAM-A
MAPK
Dimer
FGF-2
α-JAM-A
sJAM-A
shedding
sJAM-A dimer
FGF-2
Gene trascription
ADAM17
Dimer
C
TJP1
paracellular interaction
VEGFA
FGF-2
ADAMTS1
BASAL
shedding
TJP1
APICAL
Cell adhesion
Invasiveness
Proliferation
Drug resistance
Immune evasion
D
MAPK
ENO1
ENO1
PLG
Blood vessel development
sJAM-A
α-JAM-A
Caveolin1
ENO1
AURKA
MAPK
Monomer
Increase JAM-A

Figure 7

Supplementary Material

Supplementary Methods

Patients derived cells and MMECs isolation

Bone marrow (BM) primary endothelial cells from MM (MMECs) and MGUS (MGECs) patients were obtained and cultured as described.[1,2] Full BM blood served as source for MMECs identification. Endothelial cells were harvested by magnetic cell sorting with anti-CD31 micro-beads (Miltenyi Biotech, Hamburg, Germany) from adherent mononuclear cells cultured for three weeks as described.[2,3]

The NDMM patient cohort (70 male and 41 female), ages 60 to 73 (median 67 years) were newly diagnosed with MM.[4] The monoclonal (M) component was IgG (n=64), IgA (n=27), IgM (n=1) and κ or λ (n=12). The MGUS patients (23 male and 12 female), ages 42 to 79 (median 60.5 years), were IgG (n=20), IgA (n=8) and κ or λ (n=7). The validation cohort was composed of 201 relapsed/refractory patients (RRMM) defined as previously described[5] 129 male and 72 female), ages 54 to 69 (median 62 years) whose M component was IgG (n=124), IgA (n=58), IgM (n=3), IgD (n=2), κ or λ (n=13) and biclonal (n=1).

Cell separation and cultures procedures

BM mononuclear cells (BMMoCs) were obtained by centrifugation on Ficoll-Hypaque gradient of heparinized bone marrow (BM) aspirates[1] and maintained in Roswell Park Memorial Institute medium (RPMI)-1640 supplemented with 10% FBS. After seven days, media were collected and JAM-A measured by ELISA. MMECs were isolated from BMMoCs using anti-CD31 MACS beads (Miltenyi Biotech, Hamburg, Germany). Purified MMECs and MGECs were grown and expanded for four passages in fibronectin coated culture dishes (BD Falcon, Küsnacht, Switzerland) in endothelial basal medium (EBM-2 Lonza, Basel, Switzerland) supplemented with 5% FBS with 10ng/ml VEGF (Miltenyi Biotech, Hamburg, Germany) as previously described.[2,3] Cell population purity (>95%) was determined with a FACSCanto II flow cytometry system (Becton Dickinson-BD, San Jose, CA, USA). In functional studies, MMECs were used until the 6th passage of culture, in DMEM supplemented with 10% FBS, 2mMol L-Glutamine, 100U/ml Penicillin, 100μg/ml Streptomycin (Sigma-Aldrich, St. Louis, MO, USA). Human RPMI-8266 MM-cells were maintained in RPMI-1640 supplemented with 10% FBS and routinely tested to exclude mycoplasma contamination. To obtain MMECs conditioned media, MMECs were grown to 80% confluence in serum-free DMEM medium for 24 hours. Culture media, antibiotic/antimycotic, glutamine, trypsin/EDTA, and PBS without Ca^{2+} and Mg^{2+} were all purchased from Sigma-Aldrich (St. Louis, MO, USA).

MGECs, MMECs and MM-PCs were obtained from BM aspirates. MM-PCs were identified as the $CD138^{+}$ population within the gate of live cells. MM-PCs, MM-cell lines (RPMI-8226 and OPM-2) and

HUVECs were stained with an anti-JAM-A antibody (anti-JAM-A FITC, clone OV5B8 (BioLegend, San Diego, CA, USA). Full marrow blood was stained with anti-CD31 (WM-59, Thermo-Fisher, Waltham, Massachusetts, USA), anti-CD45 (HI30, Thermo-Fisher, Waltham, Massachusetts, USA) and anti-CD138 (MI15, BioLegend San Diego, CA, USA) and endothelial cells recognized from BM mononuclear cells as CD45 negative, CD138 negative, CD31 positive within the living population. Human RPMI-8226 and OPM-2 myeloma cell lines were obtained from the American Type Culture Collection (ATCC; Rockville, MD, USA), and cultured according to the manufacturer's instructions. MMECs, RPMI-8226 and OPM-2 cells were harvested for western blot, co-culture and FACS experiments. MMECs co-cultured with RPMI-8266 or OPM-2 cells were separated by immunoselection. Culture media were collected and analyzed with ELISA and an angiogenesis array (R&D Systems®, Minneapolis, Minnesota, USA). MMECs were immunomagnetically separated with anti-CD31 MACS beads (Miltenyi Biotech, Bergisch Gladbach, Germany).

Reverse transcriptase PCR, real-time RT-PCR

Isolated mRNA was reverse transcribed into cDNA with the iScript cDNA Synthesis Kit (Bio-Rad, Hercules, CA, USA). The mean of JAM-A mRNA expression levels in MGECs or in HUVECs were used as reference values and GAPDH as housekeeping gene. Real-time PCR was performed using the "StepOne real-time RT-PCR system" (Applied Biosystems, Foster City, CA, USA). Relative quantification of the mRNA level was evaluated using the comparative Ct method with glyceraldehyde 3-phosphate dehydrogenase (GAPDH) as reference gene and with the $2^{-\Delta\Delta CT}$ formula. qRT-PCR TaqMan probes were from Applied Biosystems (Waltham, MA, USA). Primer sequences are available in **Supplementary Table 4**. Total RNA from MMECs and MGECs was extracted using the RNeasy Mini kit (Qiagen, Milano, Italy) and the real-time was performed according to manufacturer's instructions.

Immunostaining and labeling of human tissues and cells

Consecutive sections of specimens with confluent plasma cell infiltrates were stained with the following antibodies: anti-CD138 (MI15, Dako Agilent, Waldbronn, Germany) and CD31 (ab76533, Abcam, Cambridge, UK), according to the manufacturer's instructions. Slides were evaluated by an experienced hemato-pathologist.

***Wound-healing* assay**

The wound-healing assay was performed as previously described[6]. In short, MMECs were grown until confluence on fibronectin-coated (10 mg/mL) 12 well plate and the "wound" was generated by scraping the cell monolayer with a P200 pipette tip. Cells were exposed to serum free medium (SFM) alone or admixed with increasing concentrations of human sJAM-A (100 ng/mL). MMECs were also treated with 100 μg/ml neutralizing/blocking α-JAM-A mAb (10μg/mL, clone J10.4, Sigma-Aldrich, St. Louis, MO, USA). Afterward cells were fixed with 4% paraformaldehyde and stained with crystal violet. The migrating MMECs were counted in 3 different fields of the wound area at X10 magnification with EVOS digital inverted microscope (Euroclone, Pero, MI, Italy). Cell viability was determined using the CellTiter-Glo® Luminescent Cell Viability Assay (Promega, Madison, WI, USA) according to the manufacturer's instructions.

Matrigel angiogenesis assay

As the homophilic interaction between sJAM-A and the native transmembrane JAM-A had been demonstrated[7,8], a Matrigel™ angiogenesis assay was done by placing the MMECs on Matrigel™-coated plates.[9] Pictures of the skeletonized topological parameters "mesh areas", "branching points" and "vessel length" of the angiogenic network were measured by two independent observers using a computerized image analyzer[10] and ImageJ software.[11]

Matrigel (Becton Dickinson-BD, San Jose, CA, USA) 48-well plates in MMECs-derived conditioned medium (CTRL) alone or supplemented with increasing concentrations of the soluble recombinant human JAM-A (sJAM-A), up to 100 ng/mL, (Human JAM-A/F11R Protein, Sino Biological, Beijing, PRC). MMECs were also plated in CTRL in presence of 0.5 µg/mL neutralizing/blocking α-JAM-A mAb. Pictures were acquired in three randomly chosen fields with an EVOS microscope.

Western blot

Total MMECs and MGECs protein lysates were quantified with the Bradford assay (Bio-Rad, Hercules, CA, USA) and subjected to immunoblot with primary and secondary antibodies to the following: JAM-A (cod. 4267, Sigma-Aldrich, St. Louis, MO, USA) mAb; JAM-AmAb (clone OV-5B8, BioLegend San Diego, CA, USA) beta-actin (cod. A1978, Sigma-Aldrich); and mouse and rabbit horseradish peroxidase–conjugated IgG (Bio-Rad). Immunoreactive bands were visualized by enhanced chemiluminescence (SuperSignal West Femto Maximum Sensitivity Substrate, Thermo Fisher Scientific, Waltham, MA, USA) with Gel Logic 1500 Imaging System (Eastman Kodak Co.). Bands were quantified using Kodak Molecular Imaging Software and expressed as arbitrary optical density (OD).

ELISA

Supernatants from MMECs alone or co-cultured with MM-cells were analyzed with ELISA to detect sJAM-A concentrations using a Human JAM-A ELISA Kit (R&D Systems, Minneapolis, MN, USA) following the manufacturer's instructions.

Chorioallantoic membrane assay (CAM)

Fertilized white Leghorn chicken eggs were incubated at 37°C at constant humidity. On day 3, the shell were opened and 2 to 3 mL of albumen were removed to detach the chorioallantoic membrane (CAM). On the 8th day, the CAMs were implanted with 1 mm^3 sterilized gelatin sponges (Gelfoam, Upjohn Co, MI, USA) filled with SFM alone or with 100 ng/mL of sJAM-A, or with MMECs conditioned medium (MMECs CM) in presence or absence of 100 µg/mL of neutralizing/blocking α-JAM-A mAb, or with medium of sJAM-A-treated MMECs (JAM-A CM) with or without neutralizing/blocking anti-JAM-A mAb. On the 12th day, blood vessels entering the sponges within the focal plane of the CAMs were counted and pictures taken *in embrio* at X50 (Olympus stereomicroscope).

CAMs were examined daily until day 12 and photographed *in ovo* with a stereomicroscope. Vessels entering the sponges within the focal plane of the CAM were counted by two observers in a double-blind fashion at 50x magnification and confirmed by ImageJ software.[11,12]

In vivo experiments and immunohistochemistry on mice tissues

Intratibial xenograft MM model

Twenty mice were treated with α-JAM-A mAb (Sigma-Aldrich, St. Louis, MO, USA, mouse monoclonal clone J10.4, 5 mg/kg body weight in 100 µL PBS) or with an isotype control. The administration schedule was three times per week on days 1, 4, 6, 8, 11, 13, 15 and 18. Mice were euthanized for histology on day 22 after MM-cell injection.

Subcutaneous xenograft MM model

Twenty mice (10/groups) were randomized to intraperitoneal (i.p.) α-JAM-A mAb (Sigma-Aldrich, St. Louis, MO, USA, mouse monoclonal clone J10.4) 5mg/kg body weight (in 100 µL PBS), or with an isotype control (mouse IgG polyclonal antibody 12–371) three days/week for 40 days. Tumor growth was measured twice weekly, and weights (mg=mm^3) calculated as the length (mm) × width^2 (mm^2)/2. Mice were sacrificed when the tumor weight reached ~2.5 g.

The isotype control utilized for MM xenograft model was obtained from Merck Millipore, Darmstadt, Germany.

Immunohistochemical analysis followed mAb binding was visualized using 3,3'Diaminobenzidine (DAB) as a chromogenic substrate. After deparaffinization and rehydration, the BM biopsy slides were placed in a pressure cooker in 0.01M citrate buffer (pH 6.1, DAKO, Hamburg, Germany) and heated for 3 min. Incubation with anti-JAM-A mAb (clone J3F.1, Santa Cruz, Dallas, TX, USA) was

carried out at room temperature for 1 hour. Detection was performed with the DAKO Advance system according to the manufacturer's protocol. BM involvement was assessed as the percentage of positive cells relative to the total cell count (for example 40% of nuclear cells). Bone marrow sections and subcutaneous extramedullary tumors were single or double stained for Ki67 (LS-C175347, LifeSpan BioSciences, Seattle, WA, USA), CD138 (LS-B9360, LifeSpan BioSciences, Seattle, WA, USA), JAM-A (clone J3F.1, Santa Cruz, Dallas, TX, USA), CD31 (ab76533, abcam, Cambridge, UK) and CD34 (QBEND10 clone, Abcam, Cambridge, UK), according to the manufacturer's instructions. JAM-A staining was performed by incubating samples with anti-JAM-A mAb at room temperature for 1 hour. Detection was performed with the DAKO Advance system according to the manufacturer's protocol, using DAB and Magenta chromogens. BM involvement was assessed as the percentage of positive cells relative to the total cell count (for example 40% of nuclear cells); Ki67 was assessed as the mean of 5 counts of 100 cells, from separate fields; vessel density was evaluated as number of CD31+ vascular structures per mm^2. Stained bone marrow sections were analyzed by two experienced hemato-pathologists with a Zeiss Axioskop 40 microscope equipped with a Zeiss AxioCam MRc digital camera.

Mice were housed according to the Institutional Animal Care and Use Committee of the University Medical School of Bari, following guidelines published by Kilkenny *et al.*[13] Clinical signs of toxicity were monitored daily, while body weight was measured twice weekly.[14]

Immunohistochemical analysis of the mouse BM or subcutaneous mass specimens was performed with a specific antibody against JAM-A as described. Hemoglobin content of each plug was measured using Drabkin's assay (Sigma Aldrich, St. Louis, MO, USA) and normalized to its weight.[14,15] Specifically, the angiogenesis quantification in the subcutaneous xenograft model was also performed by the hemoglobin content evaluation, a well-established tool used to assess vessel density in xenograft Matrigel sponge tumor models: in detail, assay aliquots of 50 μl of reconstituted complete medium, containing 50 U/ml heparin, are added to unpolymerized Matrigel at 4°C at a final volume of 0.6 ml. The Matrigel suspension was injected subcutaneously into the flanks of mice by using a cold syringe. At body temperature, the Matrigel polymerized to a solid gel, which became vascularized within 4-7 days in response to angiogenic substances. Pellets were removed at the end of the experiment, photographed, minced, and diluted in water to measure the hemoglobin content with a Drabkin reagent kit (Sigma-Aldrich, St. Louis, MO, USA)[9,14,16].

Measurement of cytokines and angiogenic factors

Before starting the treatment, peripheral blood samples from 20 mice were collected into EDTA-containing tubes before treatment initiation and one day before mice were euthanized. Plasma was separated by centrifugation (2,000 rpm for 20 min at 4 °C) within 1 h from blood drawing and aliquoted into multiple cryovials. Plasma samples were stored at −80 °C until use. Before analysis,

plasma samples were thawed slowly in an ice bath and all analyses were done from a one-off thaw sample. Cytokine and angiogenic factor (CAFs) were measured by using Q-Plex™ Array Human Angiogenesis Antigen (Quansys Biosciences, Logan, Utah) allowing the simultaneous quantification of the following factors: angiopoietin-2 (ANG-2), fibroblast growth factor-2 (FGF-2), hepatocyte growth factor (HGF), interleukin-8 (IL-8), platelet-derived growth factor-BB (PDGF-BB), tissue inhibitor of matrix metalloproteinase-1 and 2 (TIMP-1, TIMP-2), tumor necrosis factor-alpha (TNF-α), and vascular endothelial growth factor (VEGFA), according to the manufacturer's instructions. Secreted levels of CAFs were quantified through Q-View Software (Quansys Biosciences, Logan, Utah) in triplicate samples, and the mean results were used in biomarker analysis.

Human angiogenesis array

MMECs were cultured in SFM with or without 100 ng/ml sJAM-A for 24 hours and media were collected and concentrated to be analyzed by Human Angiogenesis Array kit (R&D Systems®, Minneapolis, Minnesota, USA) according to the manufacturer's instructions. Spots were quantified with ImageJ 5.1 Software (Bio-Rad) and values were reported as mean pixel density.

***In silico* analysis**

For further validation in a larger NDMM patient cohort, the public data set from the CoMMpass[19] longitudinal, prospective observational study (release IA12) was interrogated, provided by the Multiple Myeloma Research Foundation and downloaded from (https://research.mmrf.org). Two patient subgroups were considered, relapsed/progressed or died *versus* ongoing for PFS and died *versus* alive for OS. In detail, a supervised analysis was performed including 125 genes known to be prognostically relevant in MM, either due to GEP phenotyping[17] or angiogenetic pathway related signature.[18]

The public CoMMpass data set from the RNAseq data from 646 NDMM patients was analyzed and the cohort stratified depending on the outcome (progression-free survival - PFS and overall survival - OS *status*). Expression profiles in patients were compared who progressed or died in comparison with patients who did not. The dataset interrogation and the relative clinical information analysis were generated as part of the Multiple Myeloma Research Foundation Personalized Medicine Initiative.

Statistical analysis

The compiled clinical data forms, together with the recoded variables, were inserted into a database built with Office Excel software and analyzed with Stata SE15 software. The median value of the variable obtained in FACS of the mean fluorescence intensity (MFI) for the expression of the JAM-A surface was used as a cutting point to recode the latter as a categorical variable (JAM-A$^{high/low}$):

the highest values equal to the median of 989 were classified as JAM-A^{high}, the lowest values as JAM-A^{low}.

Kaplan–Meier curves were used to show progression-free survival (PFS) and overall survival (OS) related to higher levels of surface JAM-A expression, and log-rank were determined to evaluate the differences. PFS refers to the time elapsed from the date of enrollment in this study and the date of relapse, disease progression or death, determined from the last follow-up visit. OS refers to the time elapsed from the date of enrollment in this study and date of death from any cause. Given the population characteristics for NDMM cohort, the scanty number of failure events we could not perform a multivariate analysis for OS. Despite the significant impact on PFS at univariate analysis none of the covariates maintained a relevant effect in the implemented multivariate model (data not shown).

For RRMM cohort univariate and multivariate Cox proportional hazard models were performed to detect significant predictors (covariates chosen on the basis of the statistical significance (univariate analysis, $P \leq .05$) and of the clinical judgment; age and sex were used as adjusting variables) for OS and PFS in the patient cohort. The model applicability assumption was evaluated by the Schoenfeld test. The collinearity between the nominal covariates was tested using the Cramér's V measure. For the covariates that did not satisfy the hypothesis of proportional hazards we proceeded with stratified Cox model (with interaction and with no interaction including the Likelihood Ratio Test used to estimate model parameters). Applying the same statistical methodology, we also implemented an additional analysis by dividing the continuous MMECs JAM-A MFI values by quartile ranges across the entire cohort (n=312).

In vitro, *in embrio* and *in vivo* experimental results were expressed as individual data or as the mean ± SD and analyzed using Wilcoxon signed-rank test, Mann-Whitney U test and One-Way Anova test. Statistical analysis was performed using GraphPad Prism6 software (La Jolla, CA, USA). Analysis performed on the *in silico* data was conducted using t-test and fold change.

For *in vivo* experiments, sample size was calculated using G*Power software version 3.1.9.2 (power of 80% and 0.05 statistical level). Assuming an effect-size of 0.4 with statistical significance of $\alpha < .05$ and a power of 80%. Values <.05 deemed as statistically significant. Statistical analyses were performed with STATA/SE for Windows, version 15.

Supplementary Tables

Supplementary Table 1.

Patients characteristics, NDMM cohort.

Variable	N. patients (%)	Median Values
Median Age	111/111 (100)	67 years (60 - 73)
Sex	111/111 (100)	
Male:	70/111 (63)	
Female:	41/111 (37)	
R-ISS	111/111 (100)	
Stage I	23/111 (20.7)	
Stage II	65/111 (58.6)	
Stage III	23/111 (20.7)	
Type of MM	104/111 (93.7)	
IgG	64/104 (61.5)	
IgA	27/104 (26)	
IgM	1/104 (1)	
Light chain	12/104 (11.5)	
Genetic risk*:	106/111 (95)	
Standard risk:	57/106 (53.8)	
High risk:	49/106 (46.2)	
Hemoglobin	110/111 (99)	10.2 g/dL (9 – 11.8)
Hb <10 g/dL	51/110 (46.3)	
Kidney failure	107/111 (96.3)	
Yes:	49/107 (45.8)	
No:	58/107 (54.2)	
Bone lesions	111/111 (100)	
Yes:	78/111 (70.3)	
No:	33/111 (29.7)	

NDMM: newly diagnosed MM; R-ISS: Revised-international staging system.

*Evaluated in patients with appropriate genetic risk assessed according to Sonneveld P, *et al.*,[20] when appropriate material was available.[19]

Supplementary Table 2.

Patients characteristics, RRMM cohort.

Variable	N. patients (%)	Median Values
Median Age	201/201 (100)	62 years (54 - 69)
Sex	201/201 (100)	
Male:	129/201 (64.2)	
Female:	72/201 (35.8)	
R-ISS	201/201 (100)	
Stage I	61/201 (30.3)	
Stage II	117/201 (58.2)	
Stage III	23/201 (11.5)	
Type of MM	201/201 (100)	
IgG	124/201 (61.7)	
IgA	58/201 (28.8)	
IgM	3/201 (1.5)	
IgD	2/201 (1)	
Light chain	13/201 (6.5)	
Biclonal	1/201 (0.5)	
Genetic risk*:	183/201 (91)	
Standard risk:	115/201 (62.8)	
High risk:	68/201 (37.2)	
Hemoglobin	201/201 (100)	10.2 g/dL (9.7 – 12.8)
Hb <10 g/dL	55/201 (27.4)	
Kidney failure	201/201 (100)	
Yes:	64/201 (31.8)	
No:	137/201 (68.2)	
Bone lesions	201/201 (100)	
Yes:	131/201 (65.2)	
No:	70/201 (34.8)	
Extra medullary disease	201/201(100)	
Yes:	66 (32.8)	
No:	135 (67.2)	
PD at sampling	105/201 (52.2)	
Previous transplant	201/201 (100)	
Yes:	149/201 (74.1)	

No:	52/201 (25.9)	
IMiDs resistant	201/201 (100)	
Yes:	97/201 (48.3)	
No:	104/201 (51.7)	
PI resistant	201/201 (100)	
Yes:	89/201 (44.3)	
No:	112/201 (55.7)	
Previous Immunotherapy	16/201 (7.9)	

RRMM: relapsed/refractory MM; ISS: international staging system; PD: progressive disease; R-ISS: Revised-international staging system; IMiDs: immunomodulatory drugs; PI: proteasome inhibitor.
*Evaluated in patients with appropriate genetic risk according to Sonneveld P, *et al.*[20] when appropriate material was available[21]. PD: progressive disease, as defined by Rajikumar *et al.*[5]

Supplementary Table 3. Gene Expression profile summary comparison between survival characteristics from 646 patients divided in high- and low-expressers from CoMMpass longitudinal, prospective observational study (release IA12).

	PFS		OS	
Gene	**t-test; *P* value**	**Fold change**	**t-test; *P* value**	**Fold change**
ENO-1	5.97; <.0001	1.39	4.57 <.0001	1.43
AURKA	5.31; <.0001	1.87	4.11 <.0001	2
VEGFA	4.63; <.0001	1.31	2.43 .02	1.2
JAM-A	2.29; 0.02	1.13	2.64; <.01	1.2
TJP1	ns	ns	-2.59; <.01	0.8

PFS: progression free survival; OS: overall survival. ENO1: Enolase 1; AURKA: Aurora Kinase A; VEGFA: Vascular Endothelial Growth Factor A; JAM-A: Junctional adhesion molecule-A; TJP1: Tight junction protein-1. ns: not significant.

Supplementary Table 4. Primer sequences.

Oligo Name	Sequence 5' to 3'
AURKA f	GAAATTGGTCGCCCTC
AURKA r	TGATGAATTTGCTGTGATCC
CASK f	ATTCTCCATATCCATGTCTCCG
CASK r	TGGAAGAAATTTCATGTTACCC
ENO-1 f	GCCTCCTGCTCAAAGTCAAC
ENO-1 r	AACGATGAGACACCATGACG
F11R f	AAGTTGTCCTGTGCCTACTC
F11R r	ACCAGTTGGCAAGAAGGTCACC
LFA1 f	CACGAAGTTCAAGGTCAGCA
LFA1 r	TTGTGGTCTTCCTGGGTTTC
MLLT4 f	GCCAAGTGACAAAGGGAT
MLLT4 r	TAACTGAAGGCGGTAAAG
TJP1 f	TGCCTCCGAGAGAGATGACA
TJP1 r	CGCCAGCCACAAATATTCCG

AURKA: Aurora Kinase A; LFA-1: Lymphocyte function-associated antigen 1; CASK: Calcium/Calmodulin Dependent Serine Protein Kinase; ENO1: Enolase 1; F11R, alias for JAM-A, Junctional adhesion molecule-A; LFA-1: Lymphocyte function-associated antigen 1; MLLT4, alias for Afadin, Adherens Junction Formation Factor TJP1: Tight junction protein-1.

Supplementary references

1. Ferrucci A, Moschetta M, Frassanito MA, et al. A HGF/cMET autocrine loop is operative in multiple myeloma bone marrow endothelial cells and may represent a novel therapeutic target. *Clin Cancer Res Off J Am Assoc Cancer Res*. 2014;20(22):5796-5807. doi:10.1158/1078-0432.CCR-14-0847
2. Schellerer VS, Croner RS, Weinländer K, Hohenberger W, Stürzl M, Naschberger E. Endothelial cells of human colorectal cancer and healthy colon reveal phenotypic differences in culture. *Lab Investig J Tech Methods Pathol*. 2007;87(11):1159-1170. doi:10.1038/labinvest.3700671
3. Leone P, Di Lernia G, Solimando AG, et al. Bone marrow endothelial cells sustain a tumor-specific CD8+ T cell subset with suppressive function in myeloma patients. *Oncoimmunology*. 2019;8(1):e1486949. doi:10.1080/2162402X.2018.1486949
4. Rajkumar SV, Dimopoulos MA, Palumbo A, et al. International Myeloma Working Group updated criteria for the diagnosis of multiple myeloma. *Lancet Oncol*. 2014;15(12):e538-548. doi:10.1016/S1470-2045(14)70442-5
5. Rajkumar SV, Harousseau J-L, Durie B, et al. Consensus recommendations for the uniform reporting of clinical trials: report of the International Myeloma Workshop Consensus Panel 1. *Blood*. 2011;117(18):4691-4695. doi:10.1182/blood-2010-10-299487
6. Solimando AG, Brandl A, Mattenheimer K, et al. JAM-A as a prognostic factor and new therapeutic target in multiple myeloma. *Leukemia*. 2018;32(3):736-743. doi:10.1038/leu.2017.287
7. Bazzoni G, Martinez-Estrada OM, Orsenigo F, Cordenonsi M, Citi S, Dejana E. Interaction of junctional adhesion molecule with the tight junction components ZO-1, cingulin, and occludin. *J Biol Chem*. 2000;275(27):20520-20526. doi:10.1074/jbc.M905251199
8. Forrest JC, Campbell JA, Schelling P, Stehle T, Dermody TS. Structure-function analysis of reovirus binding to junctional adhesion molecule 1. Implications for the mechanism of reovirus attachment. *J Biol Chem*. 2003;278(48):48434-48444. doi:10.1074/jbc.M305649200
9. Jridi I, Catacchio I, Majdoub H, et al. The small subunit of Hemilipin2, a new heterodimeric phospholipase A2 from Hemiscorpius lepturus scorpion venom, mediates the antiangiogenic effect of the whole protein. *Toxicon Off J Int Soc Toxinology*. 2017;126:38-46. doi:10.1016/j.toxicon.2016.12.001
10. Guidolin D, Vacca A, Nussdorfer GG, Ribatti D. A new image analysis method based on topological and fractal parameters to evaluate the angiostatic activity of docetaxel by using the Matrigel assay in vitro. *Microvasc Res*. 2004;67(2):117-124. doi:10.1016/j.mvr.2003.11.002
11. Collins TJ. ImageJ for microscopy. *BioTechniques*. 2007;43(1 Suppl):25-30. doi:10.2144/000112517
12. Ribatti D, Nico B, Vacca A, Presta M. The gelatin sponge-chorioallantoic membrane assay. *Nat Protoc*. 2006;1(1):85-91. doi:10.1038/nprot.2006.13
13. Kilkenny C, Browne WJ, Cuthill IC, Emerson M, Altman DG. Improving bioscience research reporting: the ARRIVE guidelines for reporting animal research. *PLoS Biol*. 2010;8(6):e1000412. doi:10.1371/journal.pbio.1000412
14. Rao L, De Veirman K, Giannico D, et al. Targeting angiogenesis in multiple myeloma by the VEGF and HGF blocking DARPin® protein MP0250: a preclinical study. *Oncotarget*. 2018;9(17):13366-13381. doi:10.18632/oncotarget.24351
15. Tsou P-S, Ruth JH, Campbell PL, et al. A novel role for inducible Fut2 in angiogenesis. *Angiogenesis*. 2013;16(1):195-205. doi:10.1007/s10456-012-9312-y
16. Margheri F, Serratì S, Lapucci A, et al. Systemic sclerosis-endothelial cell antiangiogenic pentraxin 3 and matrix metalloprotease 12 control human breast cancer tumor vascularization and development in mice. *Neoplasia N Y N*. 2009;11(10):1106-1115. doi:10.1593/neo.09934
17. Shaughnessy JD, Zhan F, Burington BE, et al. A validated gene expression model of high-risk multiple myeloma is defined by deregulated expression of genes mapping to chromosome 1. *Blood*. 2007;109(6):2276-2284. doi:10.1182/blood-2006-07-038430
18. Hose D, Moreaux J, Meissner T, et al. Induction of angiogenesis by normal and malignant plasma cells. *Blood*. 2009;114(1):128-143. doi:10.1182/blood-2008-10-184226

19. Laganà A, Perumal D, Melnekoff D, et al. Integrative network analysis identifies novel drivers of pathogenesis and progression in newly diagnosed multiple myeloma. *Leukemia*. 2018;32(1):120-130. doi:10.1038/leu.2017.197
20. Sonneveld P, Avet-Loiseau H, Lonial S, et al. Treatment of multiple myeloma with high-risk cytogenetics: a consensus of the International Myeloma Working Group. *Blood*. 2016;127(24):2955-2962. doi:10.1182/blood-2016-01-631200
21. Ross FM, Avet-Loiseau H, Ameye G, et al. Report from the European Myeloma Network on interphase FISH in multiple myeloma and related disorders. *Haematologica*. 2012;97(8):1272-1277. doi:10.3324/haematol.2011.056176

Supplementary Figure legends

Supplementary Figure 1

JAM-A is overexpressed in MM derived endothelial cells. (A) Basal mRNA expression level of JAM-A were detected in MMECs with real time RT-PCR. The mean of JAM-A mRNA expression levels in MGECs or in HUVECs were used as reference values and GAPDH as housekeeping gene. **(B)** Anti-CD34 and anti-JAM-A staining on a representative MGUS BM sample (compare to Figure 1D and main text for details). Magnification x 200, Scale bar=50 µm. **(C)** Anti-CD31/anti-JAM-A double immunohistochemistry staining on BM trephine: within the control BM lacunae (see $CD31^+$ megakaryocytes) the vessels are more distended and endothelia display a thin, uncospicuous cytoplasmic rim. CD31 (brown) highlights endothelia lining thin walled microvessels. Lumina appear to be only slightly dilated. Anti-JAM-A (in red) stains a fraction of neoplastic plasma cells, with a cytoplasmatic pattern. Magnification x 200. Scale bar = 50 µm. Red insert: magnification x 2. **(D)** Absolute JAM-A expression across the entire cohort measured with flow cytometry and displayed as mean fluorescence intensity (MFI) values. **(E)** Kaplan Meier estimator of OS across the entire cohort recoded into quartiles of surface MMECs JAM-A expression levels. The median OS estimated in subjects within the lowest quartile ($JAM\text{-}A^{Q1}$) MMECs cells at FACS was not reached whereas in subjects in the highest one ($JAM\text{-}A^{Q4}$) MMECs the median OS was 88 months (HR= 8.24, 95% CI 3.2–20.9, $P< 0.0001$; $\chi^2_{LR}=28.15$; $P< 0.0001$ upper panel). Uni- and multivariate analysis (lower panel). BM: bone marrow; MMECs: BM primary MM endothelial cells; MGECs: MGUS derived endothelial cells; MFI: mean fluorescence intensity.

Supplementary Figure 2

Primary MM derived endothelial cells enhance sJAM-A levels and JAM-A-expression on MM after direct or indirect co-culture. Experimental designs depicted on the left. **(A)** MMECs directly co-cultured with RPMI-8226 cells at 1:5 ratio (RPMI8266:MMECs) or cultured alone for 24hrs. After removing tumor cells, MMECs were harvested and JAM-A post transcription level quantified using western blotting for RPMI-8226 cells. **(B)** MMECs cells were cultured alone or co-cultured with RPMI-8226 at 1:5 ratio (RPMI-8266:MMECs) directly co-cultured and MMECs cells analyzed for JAM-A expression with flow cytometry. (**C**) sJAM-A concentration was measured in MMECs CM with ELISA. Values represent mean ± SD. n = 12 for each group. sJAM-A concentration was measured in MM CM by ELISA. Values represent mean ± SD. n = 12 for each group; cells were directly co-cultured with RPMI-8226 cells at 1:5 ratio (RPMI8266:MMECs) or cultured alone for 24hrs. Co-culture medium and medium of MMECs cultured alone were collected and sJAM-A concentration measured by ELISA. **(D)** OPM-2 cells were cultured alone or directly co-cultured with MMECs at 1:5 ratio (OPM-2:MMECs) and analyzed for JAM-A expression by WB. Results are presented as mean ± SD (n=24 NDMM derived MMECs), Mann-Whitney test. *** $P< .001$; **** $P< .0001$. MMECs: bone marrow primary MM endothelial cells; CM: conditioned medium; NDMM: newly diagnosed MM.

Supplementary Figure 3

JAM-A neutralization impair MM endothelial cells function, without affecting MMECs viability. (A) Lack of anti-JAM-A-dependent induction of cytotoxicity against the MMECs measured with flow cytometry (Vivid, left panel). Cell viability did not differ in terms of % living cells from nine independent experiments, t-Student test. **(B)** Array of 55 human angiogenesis related proteins (left), and protein list analyzed. Relative mRNA expression level of PLG, ENO-1, FGF2, VEGFA, LFA-1, TJP1, CAV1, CASK, ADAM17, AURKA **(C-L)**

were investigated comparing MMECs to MGECs with real time RT-PCR to validate the proteome profiling results, (n=24 MGUS patients derived MGECs and 24 NDMM derived MMECs). Results are presented as mean ± SD, Mann-Whitney test. **** *P*< .0001. The mean of mRNA expression levels of JAM-A in HUVECs was used as reference sample and GAPDH as housekeeping gene. Graph compares the mRNA expression of each ligand between MGECs and MMECs and it shows the most expressed ligand in each cell type setting with the lower as unit. MMECs: bone marrow primary MM endothelial cells; PLG: plasminogen; ENO1: Enolase 1; FGF-2: Fibroblast growth factor-2; VEGFA: Vascular Endothelial Growth Factor A; LFA-1: Lymphocyte function-associated antigen 1; TJP1: Tight junction protein-1; CAV1: Caveolin1; CASK: Calcium/Calmodulin Dependent Serine Protein Kinase; ADAM17: ADAM metallopeptidase domain 17; AURKA: Aurora Kinase A; MGECs: MGUS derived endothelial cells; NDMM: newly diagnosed MM. See results and discussion for additional details.

Supplementary Figure 4

Effect of anti-JAM-A treatment on systemic sJAM-A, FGF2 and VEGF levels. (A) Representative extracted tumor masses after treatment from subcutaneous tumor xenograft model. **(B)** s-JAM-A (297,6 ± 15,57 and 71.89 ± 9,24 in the ISO Control and in the α-JAM-A-treated group respectively, t-student test, *P*< .0001)**, (C)** FGF-2 (median 1500 and 253.89 in the ISO Control and in the α-JAM-A-treated group respectively, Mann-Whitney test, *P*< .0001) and **(D)** VEGF-A (42470 ± 2694 and 4070 ± 815,6 in the ISO Control and in the α-JAM-A-treated group respectively, t-student test, *P*< .0001)**,** significantly decreased in MM bearing mice after anti-JAM-A blocking antibody treatment, evaluated with ELISA. **** *P*< .0001. For one mouse there was not sufficient biological material for ELISA test available.

FGF-2: Fibroblast growth factor-2; VEGFA: Vascular Endothelial Growth Factor A; ISO: isotype control.

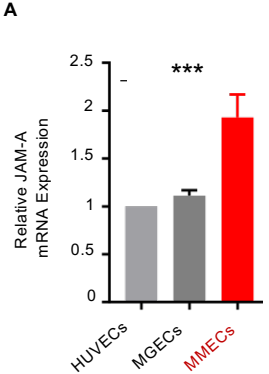

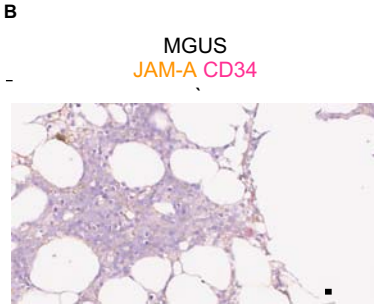

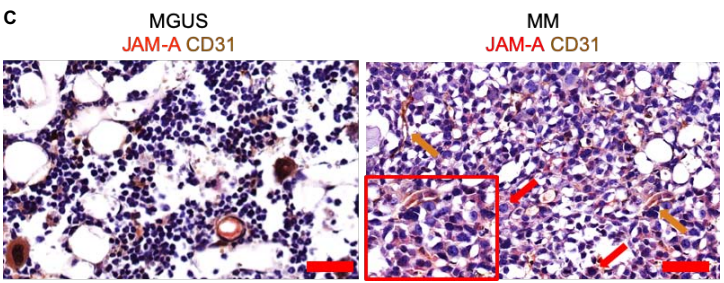

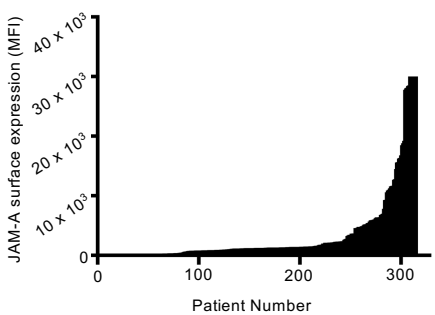

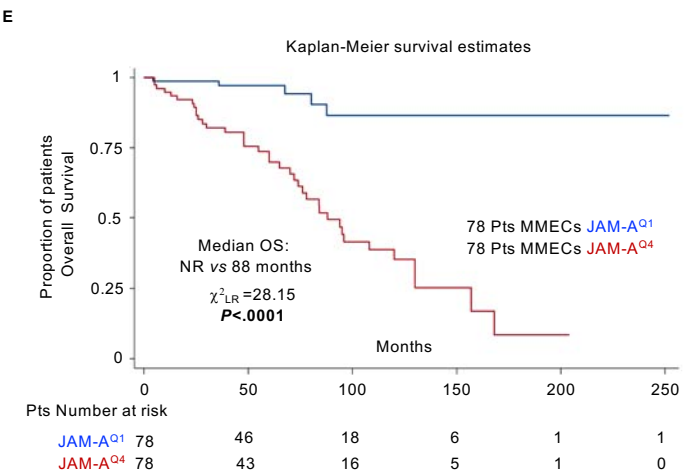

F

	*Cox model for Overall Survival			
	Univariate analysis		Multivariate analysis	
	HR (95%CI)	*P* value	HR (95%CI)	*P* value
MMECs JAM-A surface expression (JAM-A^{Q4} vs JAM-A^{Q1})	8.24 (3.24-20.96)	**<0.001**	6.36 (2.30-17.63)	**<0.001**
Bone Lesion (Yes vs No)	1.11 (0.54-2.25)	0.770	-	-
Hb (<10 vs >/-10 g/dL)	1.75 (0.96-3.19)	0.067	-	-
R-ISS				
R-Stage I	1		1	
R-Stage II	2.42 (1.04-5.61)	**0.039**	2.51 (1.01-6.22)	**0.046**
R-Stage III	2.11 (0.76-5.86)	**0.007**	2.26 (0.83-6.13)	0.106
Sex (M vs F)	1.50 (0.81-2.78)	0.191	1.84 (0.94-3.60)	0.073
Chronic kidney disease (Yes vs No)	1.88 (1.02-3.47)	**0.042**	1.85 (1.00-3.43)	**0.049**
Age	0.99 (0.96-1.03)	0.986	0.98 (0.94-1.02)	0.444

Supplementary Figure 1

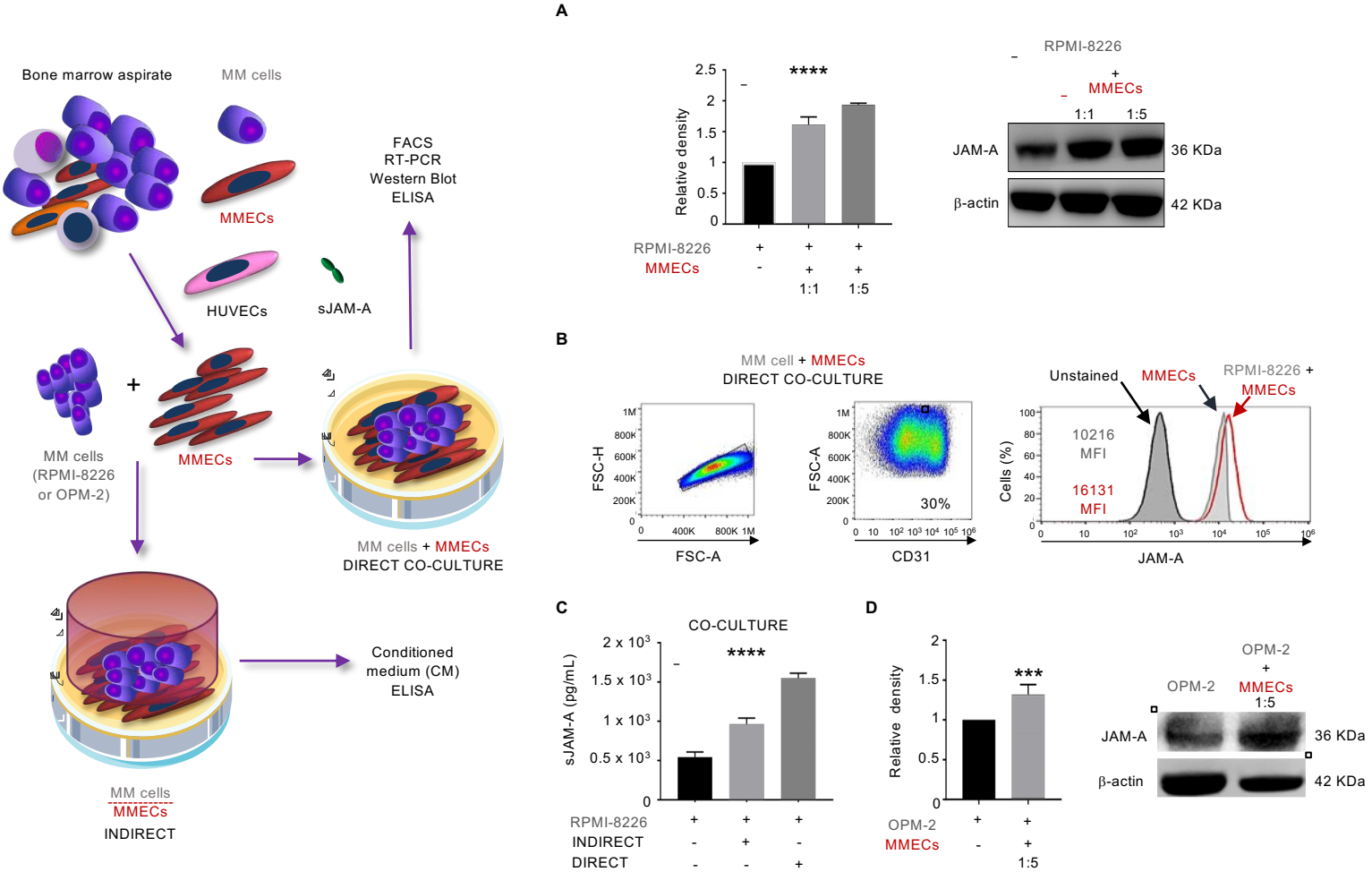

Supplementary Figure 2

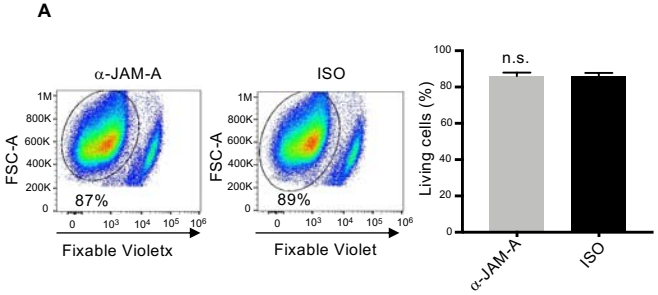

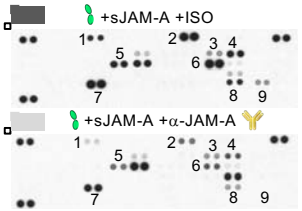

	Information	
Protein	**Alternate Nomenclature**	**Spot position**
ADAMTS-1	Human Metalloproteinase with Thrombospondin Type 1 Motifs	1
PLG	Plasmninogen	2
FGF	Fibroblast growth factor	3
FGF-2	Fibroblast growth factor basic	4
IGFBP1	Insulin Like Growth Factor Binding Protein 1	5
IL8	CXCL8	6
TIMP1	TIMP Metallopeptidase Inhibitor 1	7
VEGFA	Vascular Endothelial Growth Factor A	8
VEGFC	Vascular Endothelial Growth Factor C	9

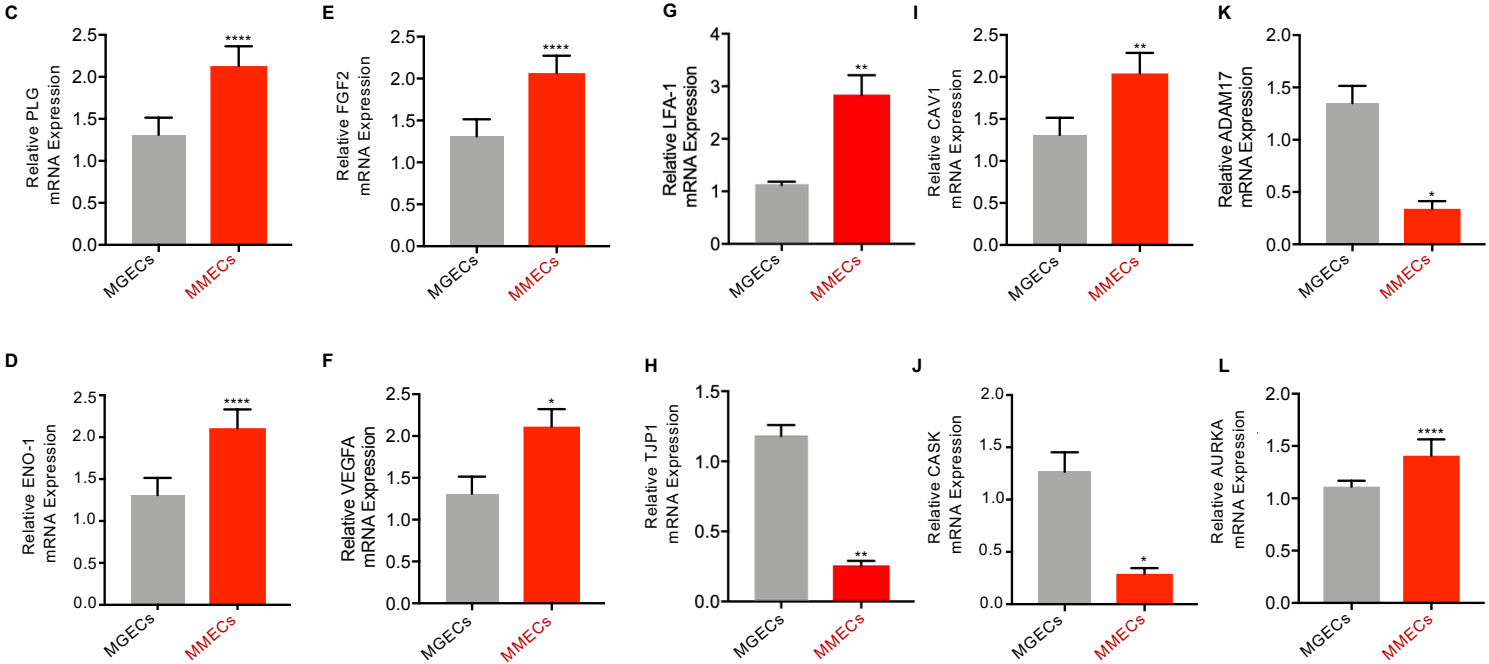

Supplementary Figure 3

A

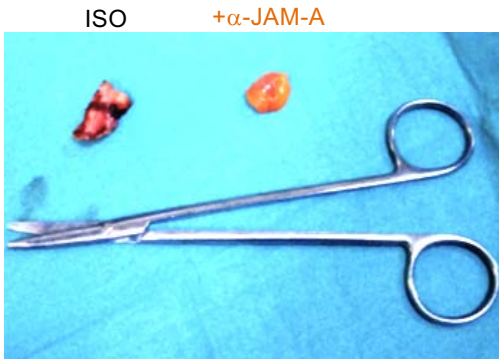

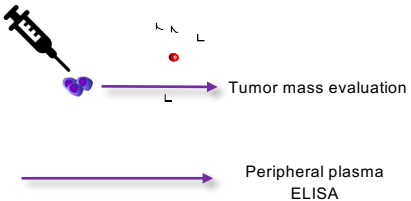

B

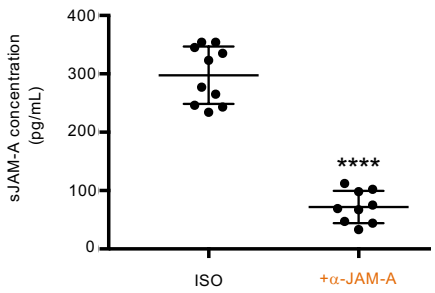

C

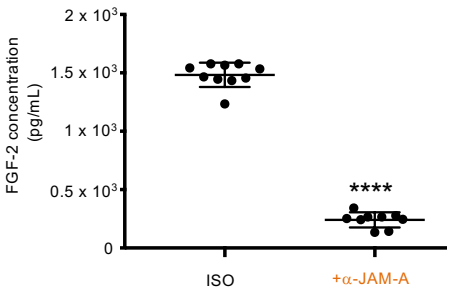

D

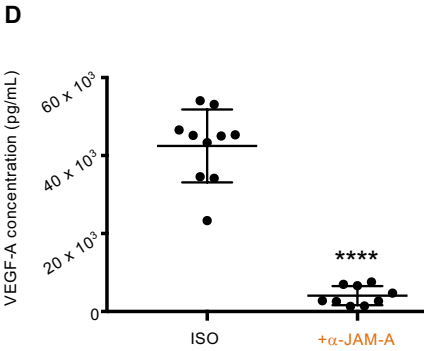

Supplementary Figure 4